The Stress-Sensing TORC2 Complex Activates Yeast AGC-Family Protein Kinase Ypk1 at Multiple Novel Sites

Kristin L. Leskoske, Françoise M. Roelants, Maria Nieves Martinez Marshall, Jennifer M. Hill, and Jeremy Thorner[1]

Division of Biochemistry, Biophysics and Structural Biology, and Division of Cell and Developmental Biology, Department of Molecular and Cell Biology, University of California, Berkeley, California 94720-3202

ABSTRACT Yeast (*Saccharomyces cerevisiae*) target of rapamycin (TOR) complex 2 (TORC2) is a multi-subunit plasma membrane-associated protein kinase and vital growth regulator. Its essential functions are exerted via phosphorylation and stimulation of downstream protein kinase Ypk1 (and its paralog Ypk2). Ypk1 phosphorylates multiple substrates to regulate plasma membrane lipid and protein composition. Ypk1 function requires phosphorylation of Thr504 in its activation loop by eisosome-associated Pkh1 (and its paralog Pkh2). For cell survival under certain stresses, however, Ypk1 activity requires further stimulation by TORC2-mediated phosphorylation at C-terminal sites, dubbed the "turn" (Ser644) and "hydrophobic" (Thr662) motifs. Here we show that four additional C-terminal sites are phosphorylated in a TORC2-dependent manner, collectively defining a minimal consensus. We found that the newly identified sites are as important for Ypk1 activity, stability, and biological function as Ser644 and Thr662. Ala substitutions at the four new sites abrogated the ability of Ypk1 to rescue the phenotypes of Ypk1 deficiency, whereas Glu substitutions had no ill effect. Combining the Ala substitutions with an N-terminal mutation (D242A), which has been demonstrated to bypass the need for TORC2-mediated phosphorylation, restored the ability to complement a Ypk1-deficient cell. These findings provide new insights about the molecular basis for TORC2-dependent activation of Ypk1.

KEYWORDS phosphorylation; TORC2; Ypk1; regulation; mutants; stress response; homeostasis

THE eukaryotic plasma membrane (PM) is a highly organized, yet dynamic, structure comprised of specific proteins and several classes of lipids (Simons and Sampaio 2011). The composition and distribution of the lipids in the PM affects many different PM-mediated processes, including endocytosis (Platta and Stenmark 2011), solute transport (Divito and Amara 2009), and signal transduction (Groves and Kuriyan 2010). Eukaryotic cells have evolved, therefore, mechanisms to sense and respond to environmental stresses that affect PM status, such as fluctuations in temperature or osmolarity, and other perturbations, such as sphingolipid limitation, and thereby adjust cell physiology appropriately to maintain homeostasis.

doi: https://doi.org/10.1534/genetics.117.1124
Manuscript received June 21, 2017; accepted for publication July 16, 2017; published Early Online July 26, 2017.
Available freely online through the author-supported open access option.
[1]Corresponding author: Division of Biochemistry, Biophysics and Structural Biology, Department of Molecular and Cell Biology, University of California at Berkeley, Rm. 526, Barker Hall, Berkeley, CA 94720-3202. E-mail: jthorner@berkeley.edu

Using budding yeast (*Saccharomyces cerevisiae*) as the experimental organism, it has been shown by us (Roelants *et al.* 2011, 2017; Muir *et al.* 2014, 2015; Alvaro *et al.* 2016) and others (Berchtold and Walther 2009; Berchtold *et al.* 2012; Niles *et al.* 2012; Sun *et al.* 2012; Fröhlich *et al.* 2016) that the large multi-subunit protein kinase target of rapamycin (TOR) complex 2 (TORC2) plays an essential role in sensing and ensuring maintenance of PM homeostasis. TORC2 is one of two evolutionarily conserved TOR-containing protein complexes (Kunz *et al.* 1993; Helliwell *et al.* 1994; Loewith *et al.* 2002; Wedaman *et al.* 2003). TORC1 is sensitive to inhibition by rapamycin, whereas TORC2 is normally insensitive to this agent (Jacinto *et al.* 2004; Huang and Manning 2009; Betz and Hall 2013; Gaubitz *et al.* 2015). In yeast, TORC2 action influences not only reactions that affect PM lipid and protein composition, but also assembly and function of the actin cytoskeleton and actin-driven endocytosis (Bartlett and Kim 2014; Gaubitz *et al.* 2016; Roelants *et al.* 2017). The catalytic subunit of the TORC1 and TORC2 complexes is a very large TOR polypeptide; metazoans possess a

single TOR-encoding gene [human mammalian TOR (mTOR), 2549 residues], whereas budding yeast (Heitman *et al.* 1991), fission yeast (Ikai *et al.* 2011), and other fungi (Eltschinger and Loewith 2016) encode two TOR proteins, Tor1 and Tor2 (2470 and 2474 residues, respectively, in *S. cerevisiae*). TORC1 is functional when its catalytic subunit is either Tor1 or Tor2, whereas only Tor2 can serve as the catalytic subunit in TORC2 (Loewith *et al.* 2002; Wedaman *et al.* 2003). The small β-propeller protein Lst8 binds tightly to and greatly stabilizes the kinase fold in both Tor1 and Tor2 (Yang *et al.* 2013; Aylett *et al.* 2016; Baretić *et al.* 2016), and thus is present in both TORC1 and TORC2. Aside from Lst8, however, the other known subunits in TORC2, namely Avo1, Avo2, Avo3/Tsc11, Bit2, Bit61, Slm1, and Slm2, are all separate and distinct from those in TORC1 (Loewith and Hall 2011; Eltschinger and Loewith 2016). Recent structural, genetic, and biochemical analysis revealed that TORC2 is only insensitive to rapamycin because the C terminus of Avo3 (mammalian homolog is Rictor) blocks the ability of rapamycin-bound FKBP12 (Fpr1 in *S. cerevisiae*) to bind to the FRB domain of Tor2; deleting a portion of the Avo3 C terminus renders TORC2 sensitive to rapamycin inhibition (Gaubitz *et al.* 2015). In a yeast cell where such an *avo3* truncation is combined with a dominant point mutation (*TOR1-1*) in the FRB domain of Tor1 which blocks its association with rapamycin-Fpr1 (Heitman *et al.* 1991), TORC2 can be uniquely inhibited by the addition of rapamycin (Gaubitz *et al.* 2015).

TORC2 is localized at the PM (Kunz *et al.* 2000; Berchtold and Walther 2009; Niles *et al.* 2012) and responds to activating perturbations and stresses by directly phosphorylating and thereby stimulating the activity of the downstream AGC-family protein kinase Ypk1 and its paralog Ypk2/Ykr2 (Chen *et al.* 1993), which are orthologs of mammalian SGK1 (Casamayor *et al.* 1999). An allele of Ypk2 (Ypk2^{D239A}) (Kamada *et al.* 2005), or a corresponding Ypk1 allele (Ypk1^{D242A}) (Roelants *et al.* 2011), which does not require TORC2-mediated phosphorylation for full activity, rescues the lethality of a *tor2* temperature-sensitive mutation at restrictive temperatures (Roelants *et al.* 2011), indicating that the functions of TORC2 required for viability are all exerted through the action of Ypk1 and/or Ypk2. Because a *YPK1*$^+$ *ypk2*Δ strain exhibits no deleterious phenotype (Chen *et al.* 1993; Roelants *et al.* 2002), Ypk1 alone is able to execute all of the essential functions carried out by these enzymes. Indeed, subsequent analysis of the substrates of Ypk1 has shown that this protein kinase maintains PM homeostasis in multiple ways. Ypk1 reduces the rate of aminoglycerophospholipid flipping from the outer to the inner leaflet of the PM by phosphorylating and inhibiting two protein kinases, Fpk1 and Fpk2, which stimulate the P-type ATPases ("flippases") that catalyze this inward translocation (Roelants *et al.* 2010). Ypk1-mediated inhibition of Fpk1 and Fpk2 also impedes endocytosis by alleviating their inhibition of the protein kinase Akl1, which phosphorylates and blocks the function of several actin patch-associated proteins (Roelants *et al.* 2017). Ypk1-mediated phosphorylation also blocks the ability of certain endocytic adaptors (α-arrestins) to promote internalization of integral PM proteins (Alvaro *et al.* 2016). Ypk1 increases metabolic flux into sphingolipid synthesis by phosphorylating and thereby relieving the inhibition exerted by two ER-localized tetraspanins (Orm1 and Orm2) on the enzyme (L-serine:palmitoyl-CoA acyltransferase) that catalyzes the first reaction in sphingolipid biosynthesis (Roelants *et al.* 2011). Moreover, Ypk1 promotes production of complex sphingolipids by phosphorylating and stimulating the activity of the catalytic subunits (Lac1 and Lag1) of the ceramide synthase complex (Muir *et al.* 2014). Unlike other stresses, hyperosmotic shock rapidly inactivates TORC2–Ypk1 signaling (Lee *et al.* 2012; Muir *et al.* 2015). As a result, the inhibitory phosphorylation that Ypk1 normally exerts on the glycerol-3P hydrogenase isoform Gpd1 is alleviated (Lee *et al.* 2012) and, similarly, the Ypk1-mediated, channel-opening phosphorylation of the aquaglyceroporin Fps1 is prevented (Muir *et al.* 2015), promoting accumulation of intracellular glycerol and cell survival.

As observed for other AGC-family protein kinases (Pearce *et al.* 2010), activation of Ypk1 is regulated by phosphorylation on residues situated within three conserved sequences. First, phosphorylation of Ypk1 on its activation loop (T-loop) at Thr504 within a conserved T^{504}FCGTPEY motif is required for basal Ypk1 activity; this modification is installed by the eisosome-associated protein kinases Pkh1 and Pkh2 (Roelants *et al.* 2002, 2004) [orthologs of mammalian 3-phosphoinositide-dependent protein kinase PDK1 (Casamayor *et al.* 1999)]. However, for cell survival in response to certain stresses (*e.g.*, sphingolipid depletion, heat shock, or hypotonic conditions), Ypk1 activity must be upregulated further by phosphorylation at Thr662 in a shorter conserved sequence F/W-T^{662}-F/Y near its C terminus (Roelants *et al.* 2004, 2011; Kamada *et al.* 2005; Berchtold *et al.* 2012; Niles *et al.* 2012; Sun *et al.* 2012), dubbed the hydrophobic motif. As first revealed by analysis of Ypk2, phosphorylation at the hydrophobic motif is mediated by TORC2, which also phosphorylates another C-terminal site (Ser644 in Ypk1) within another conserved sequence (P-V/I-DS^{644}VV-D/N-E/D), dubbed the turn motif (Roelants *et al.* 2004; Kamada *et al.* 2005). Thus, TORC2 plays a key role in stimulating Ypk1 activity, thereby allowing cells to cope with these stresses.

Given its importance in activating Ypk1 function, we sought to characterize TORC2-mediated phosphorylation of Ypk1 in greater detail. In so doing, we discovered that TORC2 phosphorylates Ypk1 at several previously uncharacterized C-terminal sites distinct from the "classical" turn and hydrophobic motifs. As we document here, phosphorylation at these additional sites is essential for full Ypk1 function. Our findings further suggest that differential phosphorylation by TORC2 at this collection of sites may provide a means for modulating the activity of the population of Ypk1 molecules in a graded manner, thereby allowing for dynamic adjustment of the level of Ypk1 activity to match the immediate needs of the cell.

Materials and Methods

Construction of yeast strains and growth conditions

S. cerevisiae strains used in this study are described in Table 1. Yeast cultures were grown in standard rich (YP) medium or in defined minimal (SC) medium (Sherman *et al.* 1986) containing 2% dextrose/glucose and were supplemented with the appropriate nutrients to permit growth of auxotrophs and/or to select for plasmids. For expression of a gene under the control of a galactose-inducible promoter, cells were grown in the appropriate SC medium containing 2% raffinose-0.2% sucrose and induced by addition of 2% galactose for 3 hr. Cultures were grown at 30° unless indicated otherwise.

Plasmids and recombinant DNA methods

Plasmids used in this study (Table 2) were constructed using standard procedures in *Escherichia coli* strain DH5α (Sambrook *et al.* 1989). All PCR reactions were performed using Phusion High-Fidelity DNA Polymerase (New England Biolabs, Beverly, MA). Site-directed mutagenesis was performed with appropriate mismatch oligonucleotide primers using the QuickChange method (Agilent Technologies), according to the manufacturer's recommendations. The fidelity of all constructs was verified by DNA sequence analysis performed in the University of California Berkeley DNA Sequencing Facility.

Cell extract preparation and immunoblotting

Samples (1.5 ml) of exponentially growing cells were harvested by brief centrifugation and stored at −80°. Cell pellets were thawed on ice; lysed in 150 μl 1.85 M NaOH, 7.4% β-mercaptoethanol; and proteins in the resulting lysate were precipitated by addition of 150 μl 50% trichloroacetic acid on ice for 10 min. Precipitated proteins were pelleted by centrifugation and washed twice with ice-cold acetone. The pellets were solubilized in a volume of 0.1 M Tris, 5% SDS to yield a final concentration representing an amount of the initial cell culture of $A_{600\ nm}$ = 0.025 per μl, and then 5× SDS sample buffer was added to a final concentration of 1×. For samples subjected to phosphatase treatment, the precipitated protein was solubilized in 100 μl solubilization buffer (125 mM sorbitol, 180 mM Tris base, 42 mM NaCl, 10.5 mM $MgCl_2$, 420 μM EDTA, 4% SDS, 2% β-mercaptoethanol), diluted with 900 μl 50 mM Tris-HCl (pH 8.5), and treated with 45 U of calf intestinal alkaline phosphatase (New England Biolabs) at 37° for 2 hr. After treatment, proteins were recollected by trichloroacetic acid precipitation and resuspended in 0.1 M Tris, 5% SDS as described above. Once solubilized, samples to be analyzed by SDS-PAGE were boiled for 10 min. Extracts containing Ypk1-myc were resolved by Phos-tag SDS-PAGE (Kinoshita *et al.* 2015) in 8% acrylamide containing 35 μM Phos-tag affinity reagent (Wako Chemicals). To resolve 3XFLAG-Orm1 isoforms, extracts were analyzed by SDS-PAGE using 10% gels containing an acrylamide:bis-acrylamide ratio of 75:1 run at 70 V (Roelants *et al.* 2010). Resolved proteins were transferred electrophoretically to a nitrocellulose membrane. The resulting membranes were blocked by incubation in Odyssey buffer (LI-COR) diluted 1:1 with PBS or TBS, then probed by incubation with an appropriate primary antibody (at the indicated dilution): mouse anti-c-myc mAb 9E10 (1:100; Monoclonal Antibody Facility, Cancer Research Laboratory, University of California, Berkeley); mouse anti-FLAG M2 (1:10,000; Sigma-Aldrich); rabbit anti-phospho-Thr662 Ypk1 (1:20,000; gift from Ted Powers, University of California, Davis); mouse anti-HA.11 (1:1000; BioLegend); rabbit polyclonal anti-Avo3 (1:100; this laboratory); goat anti-Tor2 antibodies (1:1000; Santa Cruz Biotechnology, Dallas, TX); and rabbit anti-phospho-Thr256 SGK1 (1:1000; Santa Cruz Biotechnology), which detects the equivalent site (phospho-Thr504) in Ypk1. After washing, filter-bound immune complexes were detected by incubation with an appropriate infrared dye-labeled secondary antibody—CF770-conjugated goat anti-mouse IgG (Biotium), IRDye800CW-conjugated goat anti-rabbit IgG, or IRDye680RD-conjugated goat anti-mouse IgG (Li-Cor) —diluted 1:10,000 in a 1:1 mixture of Odyssey buffer with either PBS or TBS containing 0.1% Tween 20 and 0.02% SDS. After washing, immunoblots were analyzed using an infrared imaging system (Odyssey, LI-COR).

Identification of phosphorylation sites by mass spectrometry

Ypk1 was isolated from yeast extracts by immunoprecipitation; converted to peptide fragments by protease digestion, from which phospho-peptides were enriched by adsorption to $Ti(O)_2$, as described previously (Huber *et al.* 2009); and then analyzed by mass spectrometry (MS) on an Orbitrap mass spectrometer (Thermo Fisher Scientific); all by minor modifications of procedures described in detail elsewhere (Breslow *et al.* 2010).

Immunoprecipitation of TORC2

A culture (1 L) of yeast cells expressing Avo3-3C-3XFLAG (yNM695) was grown in YPD to midexponential phase and harvested by centrifugation. Cells were washed once in 2× TNEGT buffer [100 mM Tris, pH 7.6, 300 mM NaCl, 20% glycerol, 0.24% Tergitol, 2 mM EDTA, 2 mM $NaVO_4$, 10 mM NaF, 10 mM Na-PPi, 10 mM β-glycerol phosphate, and 1× Roche Complete Protease Inhibitor tablet (Roche, Basel, Switzerland)], then resuspended in 4 ml of 2× TNEGT buffer, and frozen in droplets in liquid nitrogen. The cells were lysed cryogenically using a Mixer Mill MM301 (Retsch, Düsseldorf, Germany). After the lysate was thawed on ice, 8 ml 1× TNEGT buffer [50 mM Tris, pH 7.6, 150 mM NaCl, 10% glycerol, 0.12% Tergitol, 1 mM EDTA, 2 mM $NaVO_4$, 10 mM NaF, 10 mM Na-PPi, 10 mM β-glycerol phosphate, 1× Roche Complete Protease Inhibitor tablet (Roche)] was added and the lysate was clarified by centrifugation at 2000 × *g* for 15 min. tcgqz complexes, marked by the tightly bound Avo3-3C-3XFLAG subunit, were collected by immunoabsorption to 60 μl of mouse anti-FLAG antibody coupled-agarose resin (Sigma-Aldrich) equilibrated in 1× TNEGT buffer for 2 hr at 4°. The resin

Table 1 *S. cerevisiae* strains used in this study

Strain	Genotype	Source or reference
BY4741	*MAT***a** *his3Δ1 leu2Δ0 met15Δ0 ura3Δ0*	Research Genetics
BY4742	*MATα his3Δ1 leu2Δ0 lys2Δ0 ura3Δ0*	Research Genetics
akl1Δ	BY4742 *akl1Δ::KanMX*	Research Genetics
atg1Δ	BY4742 *atg1Δ::KanMX*	Research Genetics
ark1Δ	BY4742 *ark1Δ::KanMX*	Research Genetics
bck1Δ	BY4742 *bck1Δ::KanMX*	Research Genetics
bub1Δ	BY4742 *bub1Δ::KanMX*	Research Genetics
chk1Δ	BY4742 *chk1Δ::KanMX*	Research Genetics
cka1Δ	BY4742 *cka1Δ::KanMX*	Research Genetics
cka2Δ	BY4742 *cka2Δ::KanMX*	Research Genetics
cmk1Δ	BY4742 *cmk1Δ::KanMX*	Research Genetics
cmk2Δ	BY4742 *cmk2Δ::KanMX*	Research Genetics
ctk2Δ	BY4742 *ctk2Δ::KanMX*	Research Genetics
ctk3Δ	BY4742 *ctk3Δ::KanMX*	Research Genetics
dbf2Δ	BY4742 *dbf2Δ::KanMX*	Research Genetics
dbf20Δ	BY4742 *dbf20Δ::KanMX*	Research Genetics
dun1Δ	BY4742 *dun1Δ::KanMX*	Research Genetics
fmp48Δ	BY4742 *fmp48Δ::KanMX*	Research Genetics
hrk1Δ	BY4742 *hrk1Δ::KanMX*	Research Genetics
ime2Δ	BY4742 *ime2Δ::KanMX*	Research Genetics
ire1Δ	BY4742 *ire1Δ::KanMX*	Research Genetics
isr1Δ	BY4742 *isr1Δ::KanMX*	Research Genetics
kcc4Δ	BY4742 *kcc4Δ::KanMX*	Research Genetics
kin1Δ	BY4742 *kin1Δ::KanMX*	Research Genetics
hsl1Δ	BY4742 *hsl1Δ::KanMX*	Research Genetics
mck1Δ	BY4742 *mck1Δ::KanMX*	Research Genetics
mrk1Δ	BY4742 *mrk1Δ::KanMX*	Research Genetics
mkk2Δ	BY4742 *mkk2Δ::KanMX*	Research Genetics
kns1Δ	BY4742 *kns1Δ::KanMX*	Research Genetics
kss1Δ	BY4742 *kss1Δ::KanMX*	Research Genetics
mek1Δ	BY4742 *mek1Δ::KanMX*	Research Genetics
ptk2Δ	BY4742 *ptk2Δ::KanMX*	Research Genetics
rck1Δ	BY4742 *rck1Δ::KanMX*	Research Genetics
rim11Δ	BY4742 *rim11Δ::KanMX*	Research Genetics
ptk1Δ	BY4742 *ptk1Δ::KanMX*	Research Genetics
mkk1Δ	BY4742 *mkk1Δ::KanMX*	Research Genetics
npr1Δ	BY4742 *npr1Δ::KanMX*	Research Genetics
env7Δ	BY4742 *env7Δ::KanMX*	Research Genetics
yck1Δ	BY4742 *yck1Δ::KanMX*	Research Genetics
ypk3Δ	BY4742 *ypk3Δ::KanMX*	Research Genetics
ssk22Δ	BY4742 *ssk22Δ::KanMX*	Research Genetics
ypl150wΔ	BY4742 *ypl150wΔ::KanMX*	Research Genetics
yck2Δ	BY4742 *yck2Δ::KanMX*	Research Genetics
swe1Δ	BY4742 *swe1Δ::KanMX*	Research Genetics
sks1Δ	BY4742 *sks1Δ::KanMX*	Research Genetics
frk1Δ	BY4742 *frk1Δ::KanMX*	Research Genetics
yck3Δ	BY4742 *yck3Δ::KanMX*	Research Genetics
sps1Δ	BY4742 *sps1Δ::KanMX*	Research Genetics
sky1Δ	BY4742 *sky1Δ::KanMX*	Research Genetics
ypk2Δ	BY4742 *ypk2Δ::KanMX*	Research Genetics
rtk1Δ	BY4742 *rtk1Δ::KanMX*	Research Genetics
slt2Δ	BY4742 *slt2Δ::KanMX*	Research Genetics
skm1Δ	BY4742 *skm1Δ::KanMX*	Research Genetics
yak1Δ	BY4742 *yak1Δ::KanMX*	Research Genetics
elm1Δ	BY4742 *elm1Δ::KanMX*	Research Genetics
sat4Δ	BY4742 *sat4Δ::KanMX*	Research Genetics
smk1Δ	BY4742 *smk1Δ::KanMX*	Research Genetics
tos3Δ	BY4742 *tos3Δ::KanMX*	Research Genetics
tpk2Δ	BY4742 *tpk2Δ::KanMX*	Research Genetics
tpk3Δ	BY4742 *tpk3Δ::KanMX*	Research Genetics
vhs1Δ	BY4742 *vhs1Δ::KanMX*	Research Genetics
pkh3Δ	BY4742 *pkh3Δ::KanMX*	Research Genetics

(continued)

Table 1, *continued*

Strain	Genotype	Source or reference
*psk2*Δ	BY4742 *psk2*Δ::*KanMX*	Research Genetics
*tel1*Δ	BY4742 *tel1*Δ::*KanMX*	Research Genetics
*tor1*Δ	BY4742 *tor1*Δ::*KanMX*	Research Genetics
*tda1*Δ	BY4742 *tda1*Δ::*KanMX*	Research Genetics
*ygk3*Δ	BY4742 *ygk3*Δ::*KanMX*	Research Genetics
*gin4*Δ	BY4742 *gin4*Δ::*KanMX*	Research Genetics
*kin3*Δ	BY4742 *kin3*Δ::*KanMX*	Research Genetics
*pbs2*Δ	BY4742 *pbs2*Δ::*KanMX*	Research Genetics
*pho85*Δ	BY4742 *pho85*Δ::*KanMX*	Research Genetics
*pkh1*Δ	BY4742 *pkh1*Δ::*KanMX*	Research Genetics
*prr1*Δ	BY4742 *prr1*Δ::*KanMX*	Research Genetics
*prr2*Δ	BY4742 *prr2*Δ::*KanMX*	Research Genetics
*psk1*Δ	BY4742 *psk1*Δ::*KanMX*	Research Genetics
*ssn3*Δ	BY4742 *ssn3*Δ::*KanMX*	Research Genetics
*ste20*Δ	BY4742 *ste20*Δ::*KanMX*	Research Genetics
*tpk1*Δ	BY4742 *tpk1*Δ::*KanMX*	Research Genetics
*nnk1*Δ	BY4742 *nnk1*Δ::*KanMX*	Research Genetics
*rck2*Δ	BY4742 *rck2*Δ::*KanMX*	Research Genetics
*kin2*Δ	BY4742 *kin2*Δ::*KanMX*	Research Genetics
*ksp1*Δ	BY4742 *ksp1*Δ::*KanMX*	Research Genetics
*mlp1*Δ	BY4742 *mlp1*Δ::*KanMX*	Research Genetics
yJP544	BY4741 *hog1*Δ::*KanMX*	This laboratory
*ypk1*Δ	BY4741 *ypk1*Δ::*KanMX*	Research Genetics
*Y*FR206	BY4742 *met15*Δ*0 fpk1*Δ::*KanMX fpk2*Δ::*KanMX*	Roelants *et al.* (2010)
*fus3*Δ	BY4742 *fus3*Δ::*KanMX*	Research Genetics
*ste11*Δ	BY4742 *ste11*Δ::*KanMX*	Research Genetics
*ste7*Δ	BY4742 *ste7*Δ::*KanMX*	Research Genetics
*cla4*Δ	BY4742 *cla4*Δ::*KanMX*	Research Genetics
*kk18*Δ	BY4742 *kkq8*Δ::*KanMX*	Research Genetics
*kin4*Δ	BY4742 *kin4*Δ::*KanMX*	Research Genetics
*fpk2*Δ	BY4742 *kin82*Δ::*KanMX*	Research Genetics
*pkp2*Δ	BY4742 *pkp2*Δ::*KanMX*	Research Genetics
*gcn2*Δ	BY4742 *gcn2*Δ::*KanMX*	Research Genetics
*ssk2*Δ	BY4742 *ssk2*Δ::*KanMX*	Research Genetics
*hal5*Δ	BY4742 *hal5*Δ::*KanMX*	Research Genetics
*ctk1*Δ	BY4742 *ctk1*Δ::*KanMX*	Research Genetics
*rim15*Δ	BY4742 *rim15*Δ::*KanMX*	Research Genetics
*vps15*Δ	BY4742 *vps15*Δ::*KanMX*	Research Genetics
*bud32*Δ	BY4742 *bud32*Δ::*KanMX*	Research Genetics
*pkh2*Δ	BY4742 *pkh2*Δ::*KanMX*	Research Genetics
*snf1*Δ	BY4742 *snf1*Δ::*KanMX*	Research Genetics
*fpk1*Δ	BY4742 *fpk1*Δ::*KanMX*	Research Genetics
kin28^{ts}	BY4741 *kin28*^{ts}::*KanMX*	Costanzo *et al.* (2010)
dbf4^{ts}	BY4741 *dbf4-3*::*KanMX*	Costanzo *et al.* (2010)
ipl1^{ts}	BY4741 *ipl1-1*::*KanMX*	Costanzo *et al.* (2010)
cdc28^{ts}	BY4741 *cdc28-1*::*KanMX*	Costanzo *et al.* (2010)
rio2^{ts}	BY4741 *rio2-1*::*KanMX*	Costanzo *et al.* (2010)
pkc1^{ts}	BY4741 *pkc1-1*::*KanMX*	Costanzo *et al.* (2010)
cak1^{ts}	BY4741 *cak1-23*::*KanMX*	Costanzo *et al.* (2010)
tor2^{ts}	BY4741 *tor2-29*::*KanMX*	Costanzo *et al.* (2010)
cdc5^{ts}	BY4741 *cdc5-1*::*KanMX*	Costanzo *et al.* (2010)
cdc7^{ts}	BY4741 *cdc7-1*::*KanMX*	Costanzo *et al.* (2010)
cdc15^{ts}	BY4741 *cdc15-2*::*KanMX*	Costanzo *et al.* (2010)
sgv1^{ts}	BY4741 *sgv1-35*::*KanMX*	Costanzo *et al.* (2010)
TOR1-1 avo3$^{\Delta CT}$	*TOR1-1 avo3*Δ*1274-1430*::*HphMX6*	Gaubitz *et al.* (2015)
yKL4	BY4741 *TOR2*::*Hyg*^{R}	Muir *et al.* (2014)
yNM695	BY4741 *TOR2*::*Hyg*^{R} *AVO3-3C-3XFLAG*::*KanMX*	This laboratory
yDB344	BY4741 3XFlag-Orm1 *ypk1*Δ::Kl*URA3*	Roelants *et al.* (2011)
yAM135-A	BY4741 Ypk1(L424A)::*URA3 ypk2*Δ::*KanMX4*	Muir *et al.* (2014)

Table 2 Plasmids used in this study

Plasmid	Description	Source or reference
pRS315	*CEN*, *LEU2*, vector	Sikorski and Hieter (1989)
pFR246	pRS315 Ypk1(S51A S71A T504A S644A T662A)-myc	This study
pFR249	pRS315 Ypk1(S51A T57A S71A T504A S644A T662A)-myc	This study
pFR252	pRS315 Ypk1(S51A T57A S71A T504A S644A S653A T662A)-myc	Muir *et al.* (2015)
pFR255	pRS315 Ypk1(S51A T57A S63A S64A S71A T504A S644A S653A T662A)-myc	This study
pFR264	pRS315 Ypk1(S51A T57A S63A S64A S71A T504A S644A S653A T662A S671A S672A)-myc	Roelants *et al.* (2011)
pJEN9	pRS315 Ypk1(S51A T57A S63A S64A S71A T504A S644A S653A T662A S671A S672A S678A)-myc	This study
pKL28	pFR264 A671S	This study
pKL29	pFR264 A672S	This study
BG1805	2 μm, *URA3*, P_{GAL1}, C-terminal tandem affinity (TAP) tag vector	Open Biosystems/Dharmacon/GE Healthcare
pAX50	BG1805 Ypk1(L424A)-TAP	Muir *et al.* (2014)
pAM20	pRS315 Ypk1-myc	Roelants *et al.* (2011)
pFR221	pRS315 Ypk1(T662A)-myc	Roelants *et al.* (2011)
pFR284	pRS315 Ypk1(T662E)-myc	This study
pJEN3	pRS315 Ypk1(S653A S671A S672A S678A)-myc	This study
pJEN6	pRS315 Ypk1(S653E S671D S672E S678E)-myc	This study
pFR220	pRS315 Ypk1(S644A)-myc	This study
pFR253	pRS315 Ypk1(S653A)-myc	This study
pFR268	pRS315 Ypk1(S671A S672A)-myc	This study
pJEN8	pRS315 Ypk1(S678A)-myc	This study
pFR234	pRS315 Ypk1(D242A)-myc	This study
pKL7	pRS315 Ypk1(D242A T662A)-myc	This study
pJEN4	pRS315 Ypk1(D242A S653A S671A S672A S678A)-myc	This study
pPL215	p416 pMET25 Ypk1-3HA	Niles *et al.* (2012)
pJEN5	p416 pMET25 Ypk1(S653A S671A S672A S678A)-3HA	This study
pKL32	p416 pMET25 Ypk1(T662A)-3HA	This study
YEp352GAL	*URA3*-marked GAL promoter-containing 2 μm vector	Benton *et al.* (1994)
pFR111	YEp352GAL-Ypk1(T504A)-myc	Roelants *et al.* (2010)
pAM76	YEp352GAL-Ypk1-myc	Roelants *et al.* (2002)
pFR112	Yep352GAL-Ypk1-myc	This study
YEp351	*LEU2*-marked 2 μm vector	Hill *et al.* (1986)
pKL49	YEp351 Ypk1 (S653A S671A S672A S678A)-myc	This study

was washed four times in 1× TNEGT buffer without protease inhibitors and two times in P3C cleavage buffer (50 mM Tris, pH 7.6, 150 mM NaCl, 1 mM EDTA, 10% glycerol, 0.12% Tergitol, 1 mM DTT, 2 mM $NaVO_4$, 10 mM NaF, 10 mM Na-PPi, 10 mM β-glycerol phosphate). Avo3-3C-3XFLAG-containing TORC2 complexes were eluted by incubation with 12 U PreScission Protease (GE Healthcare, Little Chalfont, United Kingdom) in P3C buffer at 4° for 4 hr.

In vitro kinase assay

Analog-sensitive Ypk1(L424A)-TAP, expressed in yeast cells from a modified version (Dharmacon/GE Healthcare) of the vector BG1805 (Gelperin *et al.* 2005) (pAX50), was purified as described previously (Muir *et al.* 2014), incubated with either a mock immunoprecipitation or TORC2 complex isolated as described in the preceding section in 1× kinase assay buffer (20 mM Tris-HCl, pH 7.6, 50 mM NaCl, 5 mM $MgCl_2$, 1 mM PMSF, 1 mM DTT, plus 20 μM 3-MB-PP1 to block Ypk1 activity) in either the absence or presence of 250 μM NVP-BEZ235, a demonstrated inhibitor of yeast TORC2 (Kliegman *et al.* 2013). Reactions were initiated by the addition of 200 μM ATP containing 5 μCi [γ-^{32}P]ATP (PerkinElmer, Waltham, MA), incubated for 30 min at 30°, and terminated by the addition of 5× SDS-PAGE sample buffer to a 1× final concentration and boiling for 10 min. Reaction products were resolved by SDS-PAGE and analyzed by Coomassie Blue staining and by autoradiography using a Typhoon Imaging System (GE Healthcare).

Data availability

Upon request, we will freely send readily renewable research materials (*e.g.*, plasmids and strains) and reagents (*e.g.*, antibodies, if adequate supplies are available) that were generated during the course of this study to investigators at any and all not-for-profit institutions for research purposes. The authors state that all data necessary for confirming the conclusions presented in the article are represented fully within the article.

Results

Ypk1 is phosphorylated at four previously uncharacterized C-terminal sites

Prior work has documented that Ypk1 is phosphorylated at five sites by three types of protein kinases (Figure 1A). Pkh1

and its paralog Pkh2 phosphorylate Thr504 in the activation loop of the kinase fold (Casamayor *et al.* 1999; Roelants *et al.* 2002). TORC2 phosphorylates the turn (Ser644) and hydrophobic (Thr662) motifs (Roelants *et al.* 2004, 2011; Kamada *et al.* 2005; Niles *et al.* 2012). Fpk1 and its paralog Fpk2 phosphorylate Ser51 and Ser71 (Roelants *et al.* 2010) in the N-terminal negative regulatory domain (Roelants *et al.* 2002). To obtain additional insight about Ypk1 regulation, we examined whether Ypk1 is phosphorylated at any sites other than the five previously characterized. For this purpose, we expressed an epitope-tagged derivative of a mutant, Ypk1(S51A S71A T504A S644A T662A) (hereafter Ypk1^{5A}-myc) lacking the five previously characterized phosphorylation sites. To analyze the species present, we used phosphate-affinity SDS-PAGE (Phos-tag gels), which resolve phosphorylated isoforms (Kinoshita *et al.* 2015); the more highly phosphorylated a protein, the slower its mobility. We found that Ypk1^{5A}-myc exhibited multiple slower mobility bands, which were due to phosphorylation because they were nearly all removed and collapsed into a single faster mobility species upon phosphatase treatment (Figure 1B). To identify previously uncharacterized phosphorylation sites, we immunopurified native Ypk1 from cells in balanced growth and used MS to analyze the phospho-peptides present. Reassuringly, our MS analysis recovered phosphorylation at four (S71, T504, S644, and T662) of the five previously described sites in Ypk1, but many other apparent sites of phosphorylation were also detected (Figure 1C). As one means to pinpoint which sites of phosphorylation were responsible for generating which observed phospho-isoform, candidate Ser and/or Thr residues were mutated in Ypk1^{5A}-myc, alone or in combination, and the resulting effect on the migration pattern analyzed using Phos-tag gels. Although Thr57 and Ser64 were detectably phosphorylated as assessed by our MS analysis, we could observe no effect of a T57A mutation alone or combined with a S64A mutation (along with a neighboring S63A mutation) on the spectrum of species present (Figure 1D). In marked contrast, when three C-terminal residues (Ser653, Ser671, and Ser672) were mutated to Ala, each caused a readily observable loss of a specific isoform (Figure 1D). Although Ser671 was not identified as phosphorylated by MS, further analysis revealed that both Ser671 and Ser672 can be phosphorylated *in vivo*, as judged by corresponding Phos-tag gel migration shifts (Figure 1E). Because all three of these newly confirmed phosphorylation sites are located quite near the C-terminal end of Ypk1, we tested whether Ser678 was the phosphorylation site responsible for the single remaining isoform observed when all the other sites were removed from Ypk1^{5A}-myc (*i.e.*, Ypk1^{11A}-myc). Indeed, a S678A mutation (*i.e.*, Ypk1^{12A}-myc) eliminated this last slower mobility species (Figure 1D), confirming that Ser678 too can be phosphorylated *in vivo*.

As a first means to ascertain the potential biological significance of these newly identified phosphorylation sites, we aligned the amino acid sequences of the C-terminal end of *S. cerevisiae* Ypk1 with the corresponding sequence in its paralog Ypk2 and in their homologs from five *sensu stricto Saccharomyces* species, from 10 other yeast species, and from human SGK1. Not unexpectedly, we found complete conservation of the residues equivalent to the turn (S644 in Ypk1) and hydrophobic (T662 in Ypk1) motifs in all 18 proteins (Figure 2). Strikingly, however, we also found complete conservation of a phosphorylatable residue at three of the newly identified phosphorylation sites (S653, S672, and S678 in Ypk1) (Figure 2). Notably, even the sequence context surrounding these residues was also rather well conserved. Even though the most distant relatives, *e.g.*, *Schizosaccharomyces pombe* Gad8 and human SGK1, share only modest overall homology in this region with *S. cerevisiae* Ypk1, their C termini still contain putative phosphorylation sites at positions equivalent to three of those we identified. By contrast, in SGK1, Gad8, and three other yeast species, no residue equivalent to S671 in Ypk1 is present.

TORC2 is responsible for phosphorylating Ypk1 at the newly identified C-terminal sites

As an initial approach to determine which protein kinase(s) is responsible for phosphorylating Ypk1 at the new C-terminal sites, we expressed Ypk1^{5A}-myc in a targeted collection of derivatives of the yeast strain BY4741 or BY4742 that either lack the ORF (for nonessential genes) or bear a temperature-sensitive mutation (for essential genes) for 113 of the 127 protein kinases encoded in the yeast genome (Rubenstein and Schmidt 2007; Mok *et al.* 2010). We then examined the phospho-isoforms present in extracts of these cells using Phos-tag gels. Strikingly, the only mutation of a Ser/Thr protein kinase that affected phosphorylation of Ypk1^{5A}-myc was a *tor2^{ts}* allele; even at permissive temperature, Ypk1^{5A}-myc phosphorylation was markedly reduced and, after shift to the restrictive temperature, it was eliminated completely (Figure 3A). Thus, Tor2 activity is required for phosphorylation of Ypk1 at the new sites. However, Tor2 can function in either TORC1 or TORC2 (Kunz *et al.* 1993; Helliwell *et al.* 1998; Loewith *et al.* 2002; Wedaman *et al.* 2003). Hence, we examined Ypk1^{5A}-myc phosphorylation in a strain (*TOR1-1 avo3$^{\Delta CT}$*) (Gaubitz *et al.* 2015) in which TORC1 is resistant and TORC2 is susceptible to inhibition by rapamycin. We found that in the absence of rapamycin the majority of Ypk1^{5A}-myc migrated as phosphorylated (slower mobility) isoforms, whereas after treatment with rapamycin, the bulk of the Ypk1^{5A}-myc migrated as the unphosphorylated species (Figure 3B, left); indicating that, just as previously found for the turn and hydrophobic motifs, TORC2 activity is required for phosphorylation of Ypk1 at the new C-terminal sites. As an additional control, we found, in separate experiments, that Ypk1^{5A}-myc expressed in wild-type (WT) cells exhibited no change in migration pattern when treated with rapamycin (Figure 3B, right). Even though Ypk1^{5A}-myc itself is inactive (because it cannot be phosphorylated at either the activation loop or the turn and hydrophobic motifs), perhaps autophosphorylation in *trans* by endogenous Ypk1 or Ypk2 could contribute to the observed phosphorylation at the new C-terminal sites. However, we ruled out this possibility

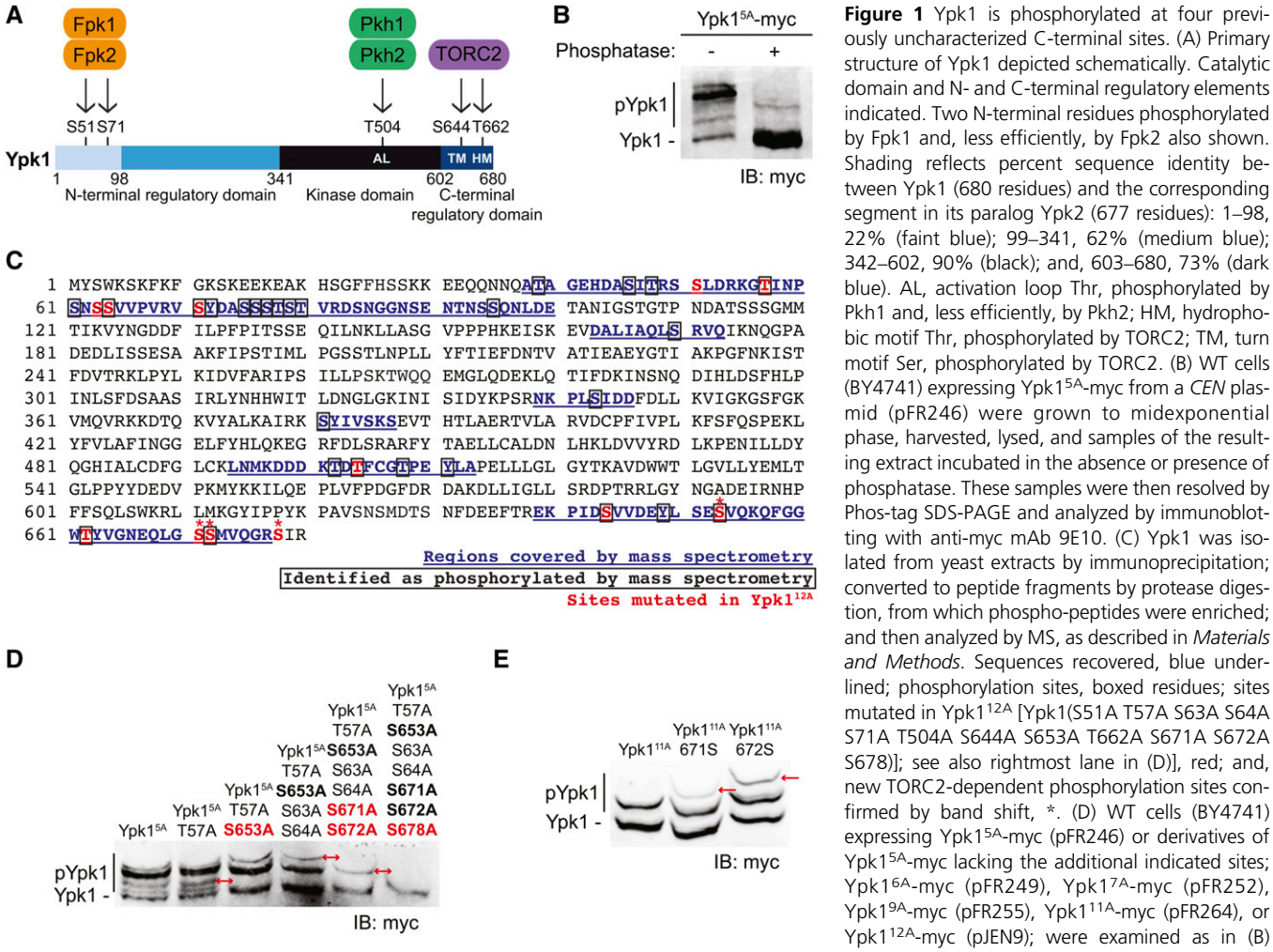

Figure 1 Ypk1 is phosphorylated at four previously uncharacterized C-terminal sites. (A) Primary structure of Ypk1 depicted schematically. Catalytic domain and N- and C-terminal regulatory elements indicated. Two N-terminal residues phosphorylated by Fpk1 and, less efficiently, by Fpk2 also shown. Shading reflects percent sequence identity between Ypk1 (680 residues) and the corresponding segment in its paralog Ypk2 (677 residues): 1–98, 22% (faint blue); 99–341, 62% (medium blue); 342–602, 90% (black); and, 603–680, 73% (dark blue). AL, activation loop Thr, phosphorylated by Pkh1 and, less efficiently, by Pkh2; HM, hydrophobic motif Thr, phosphorylated by TORC2; TM, turn motif Ser, phosphorylated by TORC2. (B) WT cells (BY4741) expressing Ypk1^{5A}-myc from a *CEN* plasmid (pFR246) were grown to midexponential phase, harvested, lysed, and samples of the resulting extract incubated in the absence or presence of phosphatase. These samples were then resolved by Phos-tag SDS-PAGE and analyzed by immunoblotting with anti-myc mAb 9E10. (C) Ypk1 was isolated from yeast extracts by immunoprecipitation; converted to peptide fragments by protease digestion, from which phospho-peptides were enriched; and then analyzed by MS, as described in *Materials and Methods*. Sequences recovered, blue underlined; phosphorylation sites, boxed residues; sites mutated in Ypk1^{12A} [Ypk1(S51A T57A S63A S64A S71A T504A S644A S653A T662A S671A S672A S678)]; see also rightmost lane in (D)], red; and, new TORC2-dependent phosphorylation sites confirmed by band shift, *. (D) WT cells (BY4741) expressing Ypk1^{5A}-myc (pFR246) or derivatives of Ypk1^{5A}-myc lacking the additional indicated sites; Ypk1^{6A}-myc (pFR249), Ypk1^{7A}-myc (pFR252), Ypk1^{9A}-myc (pFR255), Ypk1^{11A}-myc (pFR264), or Ypk1^{12A}-myc (pJEN9); were examined as in (B) without any phosphatase treatment. (E) WT cells (BY4741) expressing Ypk1^{11A}-myc (pFR264) or derivatives of Ypk1^{11A}-myc in which the indicated additional phosphorylation site was restored, Ypk1$^{11A\ 671S}$-myc (pKL28) or Ypk1$^{11A\ 672S}$-myc (pKL29), were examined as in (D). IB, immunoblot. In (D) and (E), red arrows indicate the change in the migration pattern caused by the indicated mutation(s).

because Ypk1^{5A}-myc showed no change in migration pattern when expressed in *ypk1^{as} ypk2*Δ cells, regardless of whether or not they were treated with the Ypk1^{as} inhibitor (3-MB-PP1) (Figure 3C).

Finally, to confirm, as also reported by others (Niles *et al.* 2012), that Ypk1 is a direct substrate of TORC2 *in vitro*, we purified TORC2 complexes by immuno-isolation (Figure 3D). When incubated alone, we observed robust autophosphorylation of TORC2 constituents (Figure 3E). When incubated in the presence of purified Ypk1^{as} (in the presence of 3-MB-PP1 to block its activity), we observed robust phosphorylation of Ypk1^{as}, as well as a corresponding reduction in TORC2 autophosphorylation, as expected for inhibition of autophosphorylation by the presence of a *bona fide* competing substrate (Figure 3E). Moreover, when the TORC2 inhibitor NVP-BEZ235 was added, incorporation into Ypk1 and TORC2 autophosphorylation were both greatly diminished. Thus, as expected, Ypk1 is a direct TORC2 substrate. To confirm that the observed TORC2-dependent incorporation occurred not only at S644 and T662, but also at the additional C-terminal sites in Ypk1, we attempted to purify a Ypk1^{as}(S653A S671A S672A S678A) mutant. However, as discussed in greater detail below, these mutations greatly destabilized Ypk1, making recovery of sufficient purified protein technically problematic.

Phosphorylation at the new C-terminal sites is necessary for optimal Ypk1 function

The antibiotic myriocin (Myr), also known as ISP-1 (Miyake *et al.* 1995; Ikushiro *et al.* 2004; Yeung 2011), inhibits eukaryotic cell growth because it is a transition-state mimic that potently blocks L-serine:palmitoyl-CoA C-palmitoyltransferase (decarboxylating) (EC 2.3.1.50), the first enzyme unique to the sphingolipid biosynthetic pathway (Dunn *et al.* 2004; Dickson *et al.* 2006; Megyeri *et al.* 2016; Olson *et al.* 2016). Moreover, prior work has demonstrated that Ypk1-deficient cells are hypersensitive to the growth-inhibitory action of Myr (Momoi *et al.* 2004; Roelants *et al.* 2004). Subsequent studies revealed that TORC2-stimulated, Ypk1-mediated phosphorylation of several substrates that are rate limiting for sphingolipid production is required for cell survival in

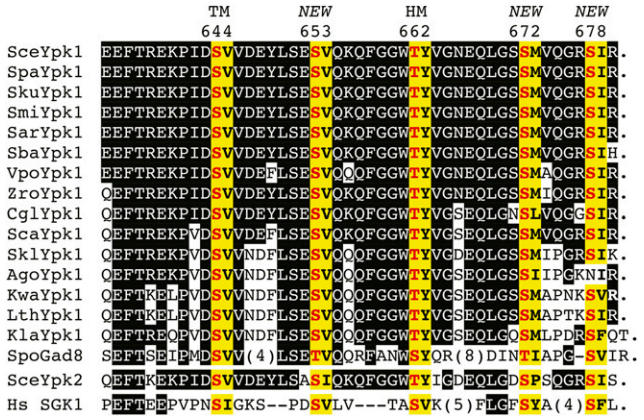

Figure 2 Sequence comparison of the C-terminal ends of Ypk1 homologs. The amino acid sequence of the C-terminal end of *S. cerevisiae* (Sce) Ypk1 (top line) was aligned with the corresponding segment of Ypk1 orthologs from the *sensu stricto* group *S. paradoxus* (Spa), *S. kudriavzevii* (Sku), *S. mikatae* (Smi), *S. arboricola* (Sar), *S. bayanus* (Sba), the more divergent species *Vanderwaltozyma polyspora* (Vpo), *Zygosaccharomyces rouxii* (Zro), *Candida glabrata* (Cgl), *S. castellii* (Sca), *S. kluyveri* (Skl), *Ashbya gossypii* (Ago), *Kluveromyces waltii* (Kwa), *Lachancea thermotolerans* (Lth), *K. lactis* (Kla), *S. pombe* (Spo), its *S. cerevisiae* paralog Ypk2, and its human (Hs) counterpart SGK1 (bottom line). To emphasize the degree of relatedness to *S. cerevisiae* Ypk1, only identities between the other proteins and *S. cerevisiae* Ypk1 are indicated (white letters on black boxes). One-residue gaps (–) and insertions of the indicated length (parentheses) were introduced to maximize the alignment of the most distant orthologs. Period (.) indicates the end of the ORF. Matches to our consensus TORC2 phospho-acceptor site motif (-S/T-Hpo-, where Hpo denotes any hydrophobic residue) (yellow boxes with phosphorylation site in bold red and hydrophobic residue in bold black). The two classical sites for TORC2-mediated phosphorylation—the so-called turn motif (TM) and hydrophobic motif (HM) (Pearce *et al.* 2010)—and the additional sites (*NEW*) discovered in this study are indicated above, along with the corresponding residue in *S. cerevisiae* Ypk1. Sequence sources were: Sce (strain S288C) from the *Saccharomyces* Genome Database (http://www.yeastgenome.org/locus/S000001609/protein); Spa, Sku, Smi, Sba, Sca, and Skl (Cliften *et al.* 2003; Kellis *et al.* 2003); Sar (GenBank EJS42953.1), Vpo (GenBank EDO19622.1), Zro (EMBL Bank CAR29179.1), and Lth (EMBL Bank CAR22493.1); Cgl, Ago, Kwa, Kla, Spo, and Sce Ypk2 from the Fungal Orthogroups database at the Broad Institute (https://portals.broadinstitute.org/cgi-bin/regev/orthogroups/show_orthogroup.cgi?orf=YKL126W); and Hs SGK1, isoform 2 (GenBank ACD35864.1).

response to sphingolipid limitation (Roelants *et al.* 2011; Berchtold *et al.* 2012; Muir *et al.* 2014). Hence, the degree of resistance to Myr provides a convenient phenotypic read out for the efficacy of Ypk1 function *in vivo*.

Therefore, to assess whether TORC2-dependent phosphorylation of Ypk1 at its C-terminal sites modulates Ypk1 function, we tested the Myr sensitivity of various unphosphorylatable and phospho-mimetic alleles of Ypk1 in *ypk1*Δ cells. As expected, a Ypk1^{T662A}-myc mutant (Figure 4A), which cannot be phosphorylated by TORC2 at the hydrophobic motif, and a Ypk1^{S644A}-myc mutant, which cannot be phosphorylated by TORC2 at the turn motif (Figure 4B), displayed much greater sensitivity to Myr than cells expressing Ypk1^{WT}-myc (Figure 4A). Similarly, a mutant lacking all four of the newly identified C-terminal phosphorylation sites [Ypk1(S653A S671A S672A S678A)-myc, hereafter Ypk1^{AAAA}-myc] exhibited increased Myr sensitivity, but at a somewhat higher concentration of this compound (Figure 4A), whereas loss of one or even two of these sites exhibited no noticeable increase in Myr sensitivity (Figure 4B), suggesting that the effects of phosphorylation at these positions may be additive in stimulating Ypk1 action. Indeed, in marked contrast to the Myr sensitivity of cells expressing Ypk1^{AAAA}-myc, a mutant in which the same four residues were mutated to Glu or Asp (Ypk1^{EDEE}-myc) supported robust growth in the presence of Myr, indicating that mimicking phosphorylation at these four sites allows for full Ypk1 function (Figure 4A).

It has been shown previously that the N-terminal mutation D242A bypasses the need for TORC2-mediated phosphorylation of Ypk1 (Roelants *et al.* 2011), suggesting that the N-terminal domain exerts some negative regulatory constraint on the C-terminal catalytic domain, in agreement with prior evidence (Roelants *et al.* 2002). Thus, it seems that the role of TORC2-mediated phosphorylation, like the D242A mutation, is to alleviate the inhibitory constraint imposed by the N-terminal domain. Consistent with that model, installing the D242A mutation in either Ypk1^{T662A}-myc or Ypk1^{AAAA}-myc fully restored their ability to support growth in the presence of Myr (Figure 4C).

To assess the effect of TORC2-dependent phosphorylation at the newly defined C-terminal sites on Ypk1 activity, we examined its ability to phosphorylate a known substrate *in vivo*. We have shown previously that Myr treatment stimulates Ypk1-mediated phosphorylation of Orm1 and that mutating a critical TORC2 target site in Ypk1 (T662) substantially reduces the ability of Ypk1 to phosphorylate Orm1 after Myr treatment (Roelants *et al.* 2011). Therefore, we monitored Ypk1-dependent phosphorylation of Orm1 after Myr treatment in cells expressing WT Ypk1 and various Ypk1 mutants. Cells expressing Ypk1^{AAAA}-myc exhibited a marked reduction in Orm1 phosphorylation in response to Myr treatment compared to cells expressing Ypk1^{WT}-myc, whereas cells expressing either Ypk1$^{D242A\ +\ AAAA}$ or Ypk1^{EDEE}-myc exhibited a level of Orm1 phosphorylation equivalent to that of WT Ypk1-myc or Ypk1^{D242A}-myc cells (Figure 4D). Collectively, these observations suggested that lack of TORC2 phosphorylation of Ypk1 at the four newly discovered sites significantly compromises Ypk1 function.

Phosphorylation at the new C-terminal sites is also necessary for Ypk1 stability

In addition to modulation of catalytic activity, phosphorylation can change protein stability or localization, which may also influence enzyme function. For this reason, we also examined whether phosphorylation of Ypk1 at the four new C-terminal sites affected its expression level by analyzing the steady-state amount of various Ypk1 unphosphorylatable and phospho-mimetic mutants by immunoblotting (Figure 5A). When extracts from untreated cells were examined by standard SDS-PAGE, Ypk1-myc migrated as a doublet; the slower mobility species represents Ypk1 isoforms phosphorylated by Fpk1 (and Fpk2), and Fpk1 and Fpk2 are themselves phosphorylated

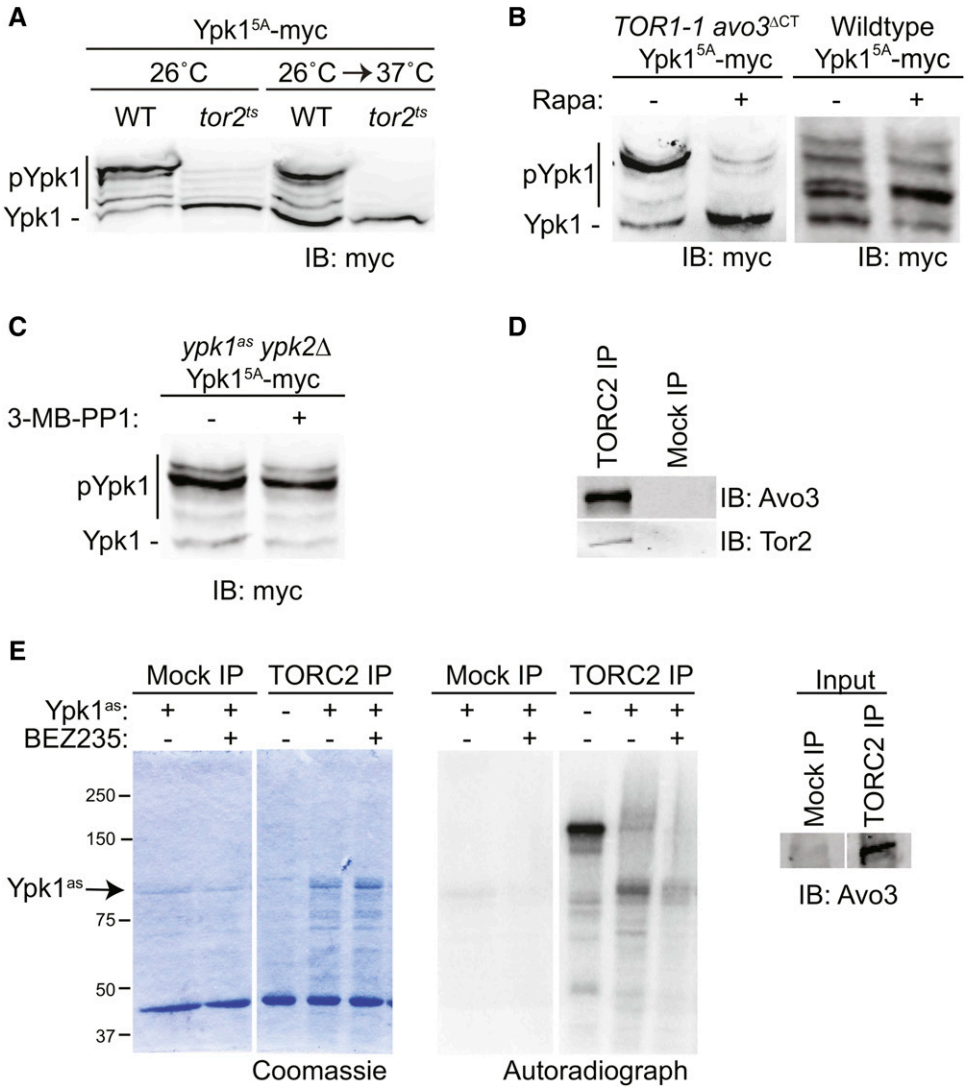

Figure 3 TORC2 phosphorylates the novel C-terminal sites. (A) WT (BY4741) or otherwise isogenic *tor2*^{ts} cells expressing Ypk1^{5A}-myc (pFR246) were grown at 26° to midexponential phase and then either kept at 26° or shifted to 37° for 2 hr, harvested, lysed, and samples of the resulting extracts resolved by Phos-tag SDS-PAGE and analyzed by immunoblotting with anti-myc mAb 9E10. (B) *TOR1-1 avo3*$^{\Delta CT}$ cells (left) expressing Ypk1^{5A}-myc (pFR246) were grown to midexponential phase, treated for 20 min with either vehicle alone (Tween 20:ethanol, 10:90) or 200 nM rapamycin in the same solvent as indicated, collected, and analyzed as in (A). WT cells (BY4741) expressing Ypk1^{5A}-myc (pFR246) (right) were treated in the same manner in a separate experiment. (C) Strain yAM135-A (*ypk1*^{as} *ypk2*Δ) expressing Ypk1^{5A}-myc (pFR246) was grown to midexponential phase and then treated with either vehicle alone (DMSO) or 10 μM 3-MB-PP1 for 1 hr, harvested, and then analyzed as in (A). (D) WT (Mock IP) (yKL4) and Avo3-3C-3XFLAG (TORC2 IP) (yNM695) strains were grown in YPD to midexponential phase, harvested, lysed, and TORC2 immunoprecipitated from the resulting extracts using anti-FLAG antibody-coupled agarose resin. Immunoprecipitated proteins were resolved by SDS-PAGE and analyzed by immunoblotting with anti-Avo3 and anti-Tor2 antibodies. (E) Mock and TORC2 preparations, as in (D), were incubated with [γ-^{32}P]ATP, either alone or in the presence of purified analog-sensitive Ypk1^{as}, in either the absence or presence of the TORC2 inhibitor NVP-BEZ235, as indicated. Reaction products were resolved by SDS-PAGE and analyzed by Coomassie staining and, after drying the gel, by autoradiography.

and inhibited by Ypk1 (Roelants *et al.* 2010). Thus, when cells are treated with Myr and Ypk1 activity is stimulated, Ypk1-dependent phosphorylation of Fpk1/Fpk2 increases, resulting in reduced Fpk-mediated phosphorylation of Ypk1. Hence, in cells treated with Myr, Ypk1-myc ran predominantly as the faster mobility species (and appeared more abundant because the signal is not as diffuse), whereas Ypk1^{T662A}-myc which prevents robust TORC2 activation of Ypk1 did not undergo this shift, but the phospho-mimetic allele Ypk1^{T662E}-myc did (Figure 5A). Moreover, as reported by others (Tanoue *et al.* 2005), mutation of the hydrophobic motif phosphorylation site (T662) did not compromise the stability of Ypk1. Strikingly, however, the level of Ypk1^{AAAA}-myc was significantly lower than that of Ypk1^{WT}-myc, Ypk1^{T662A}-myc, or Ypk1^{T662E}-myc and its pattern did not change upon Myr treatment, suggesting that TORC2-dependent phosphorylation at the four new C-terminal sites is important for both Ypk1 stability and function. Consistent with this hypothesis, under the same conditions, the level of the phospho-mimetic mutant Ypk1^{EDEE}-myc was even higher than that of Ypk1^{WT}-myc. These results indicate that the effect on Ypk1 stability is specific to the four new C-terminal sites.

Although these observations show that phosphorylation at the four new C-terminal sites is important for Ypk1 stability, two further observations demonstrate that the deficit in function of Ypk1^{AAAA} cannot be attributed to its lower level of expression. First, installation of the D242A mutation which fully restored function to Ypk1^{AAAA}-myc, as judged by both Myr resistance (Figure 4A) and efficiency of Orm1 phosphorylation (Figure 4D), did not increase the level of the protein (Figure 5B). In fact, the D242A mutation seemed to destabilize Ypk1^{WT}-myc and especially Ypk1^{T662}-myc to

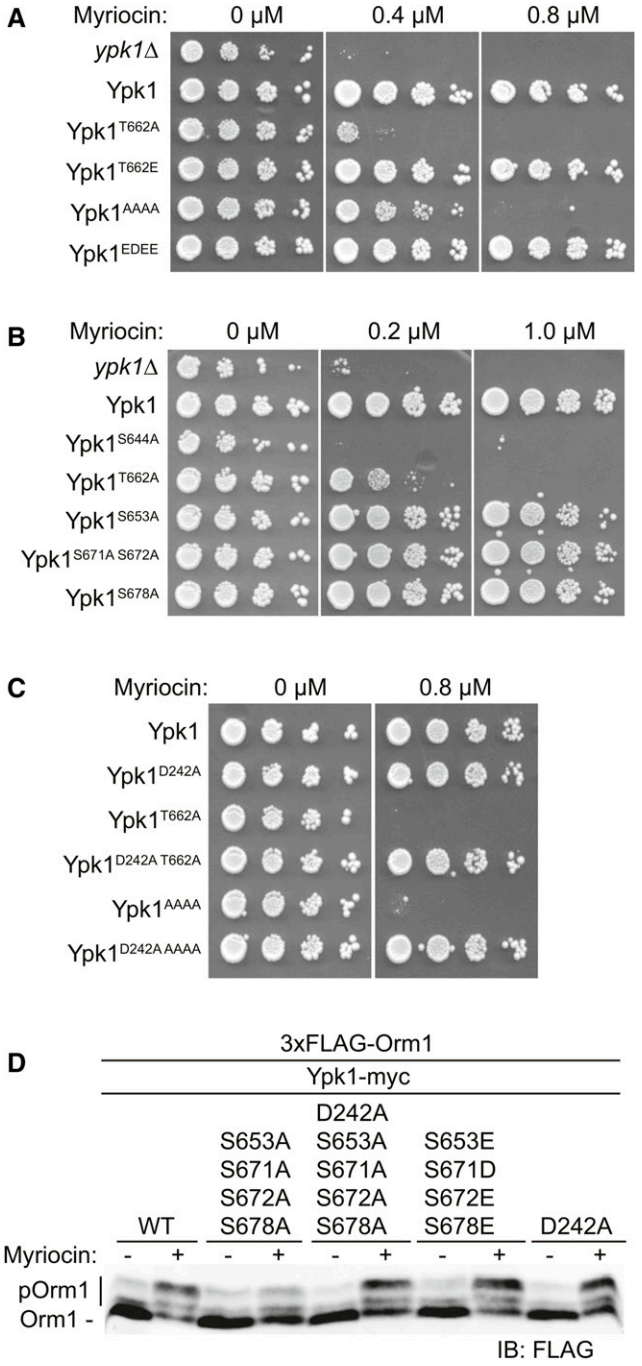

Figure 4 TORC2-dependent phosphorylation of Ypk1 at the new C-terminal sites is required for full Ypk1 function. (A) Cultures of *ypk1*Δ cells containing either empty vector (pRS315) or the same plasmid expressing Ypk1^{WT}-myc (pAM20), Ypk1^{T662A}-myc (pFR221), Ypk1^{T662E}-myc (pFR284), Ypk1$^{S653A\ S671A\ S672A\ S678A}$-myc (pJEN3), or Ypk1$^{S653E\ S671D\ S672E\ S678E}$-myc (pJEN6) were adjusted such that $A_{600\ nm}$ = 1.0 and then spotted in 10-fold serial dilutions onto SCD-Leu plates containing the indicated concentrations of Myr and incubated at 30° for 3 days. (B) Serial dilutions of *ypk1*Δ cells containing either empty vector (pRS315) or the same plasmid expressing Ypk1^{WT}-myc (pAM20), Ypk1^{S644A}-myc (pFR220), Ypk1^{T662A}-myc (pFR221), Ypk1^{S653A}-myc (pFR253), Ypk1$^{S671A\ S672A}$-myc (pFR268), or Ypk1^{S678A}-myc (pJEN8) were analyzed as in (A). (C) Cultures of *ypk1*Δ cells containing either empty vector (pRS315) or the same plasmid expressing Ypk1^{WT}-myc (pAM20), Ypk1^{D242A}-myc (pFR234), Ypk1^{T662A}-myc (pFR221), Ypk1$^{D242A\ T662A}$-myc (pKL7), Ypk1$^{S653A\ S671A\ S672A\ S678A}$-myc (pJEN3), or Ypk1$^{D242A\ 653A\ S671A\ S672A\ S678A}$-myc (pJEN4) were analyzed as in (A). (D) Strain yDB344 (3XFLAG-*ORM1 ypk1*Δ) expressing either Ypk1^{WT}-myc (pAM20), Ypk1$^{S653A\ S671A\ S672A\ S678A}$-myc (pJEN3), Ypk1$^{D242A\ S653A\ S671A\ S672A\ S678A}$-myc (pJEN4), Ypk1$^{S653E\ S671D\ S672E\ S672E}$-myc (pJEN6), or Ypk1^{D242A}-myc (pFR234) were grown to exponential phase in selective medium, treated with either vehicle (methanol) or 1.25 μM Myr for 2 hr. After harvesting, whole-cell extracts were prepared, resolved by SDS-PAGE, and analyzed by immunoblotting with anti-FLAG M2 antibody.

some degree (Figure 5B). Conversely, even when produced at an elevated level by expression from a multi-copy 2 μm DNA plasmid in an amount equivalent to WT Ypk1 (Figure 5C), Ypk1^{AAAA} was still unable to restore Myr resistance (Figure 5D). Hence, the physiological phenotypes associated with loss of phosphorylation at the new C-terminal sites arise largely from impairment of the functional activity of Ypk1.

Phosphorylation at the new C-terminal sites promotes efficient hydrophobic motif phosphorylation

Compared to absence of phosphorylation at the four newly identified C-terminal sites, absence of phosphorylation at either its turn (S644) or its hydrophobic (T662) motif is more crippling to Ypk1 function (Figure 4, A and B). Moreover, despite its much lower steady-state level compared to Ypk1^{WT}-myc (Figure 5B), Ypk1$^{D242A\ +\ AAAA}$-myc exhibited no deleterious phenotypes (Figure 4C). Therefore, we considered the possibility that, at the mechanistic level, the primary role of TORC2-mediated phosphorylation at the four new C-terminal sites is to prime Ypk1 for full activation because modification of these sites helps expose, makes more efficient, or allows for more sustained TORC2-dependent phosphorylation at the turn and hydrophobic motifs. However, for Ypk1 to be active at all, it must also be phosphorylated at Thr504 in its activation loop by Pkh1 (and Pkh2) (Casamayor *et al.* 1999; Roelants *et al.* 2002, 2004). To examine which of these sites of phosphorylation might be compromised when Ypk1 cannot be phosphorylated at the four new C-terminal sites, we used phospho-site-directed antibodies that detect specifically the Pkh1 site (P-Thr504) and the TORC2 site in the hydrophobic motif (P-Thr662). We have demonstrated before that a commercial phospho-site antibody directed against the highly homologous PDK1 site in human SGK1 robustly and specifically detects P-Thr504 in Ypk1 (Roelants *et al.* 2010). A phospho-site antibody that specifically detects P-Thr662 in Ypk1 was generated and validated by Powers and co-workers (Niles *et al.* 2012), and generously provided to us. To permit proper comparison of the level of phosphorylation in each Ypk1 variant, the volumes of extract loaded were adjusted to ensure that the total amount of Ypk1 present in each lane was equivalent. We found that, compared to Ypk1^{WT}-3HA, phosphorylation of Thr662 is abolished in Ypk1^{AAAA}-3HA down to the background level observed for a Ypk1^{T662A}-3HA mutant which totally lacks the site (Figure 6A); whereas the level of phosphorylation of Thr504 in a Ypk1$^{S644A\ T662A}$-myc mutant which lacks the TORC2

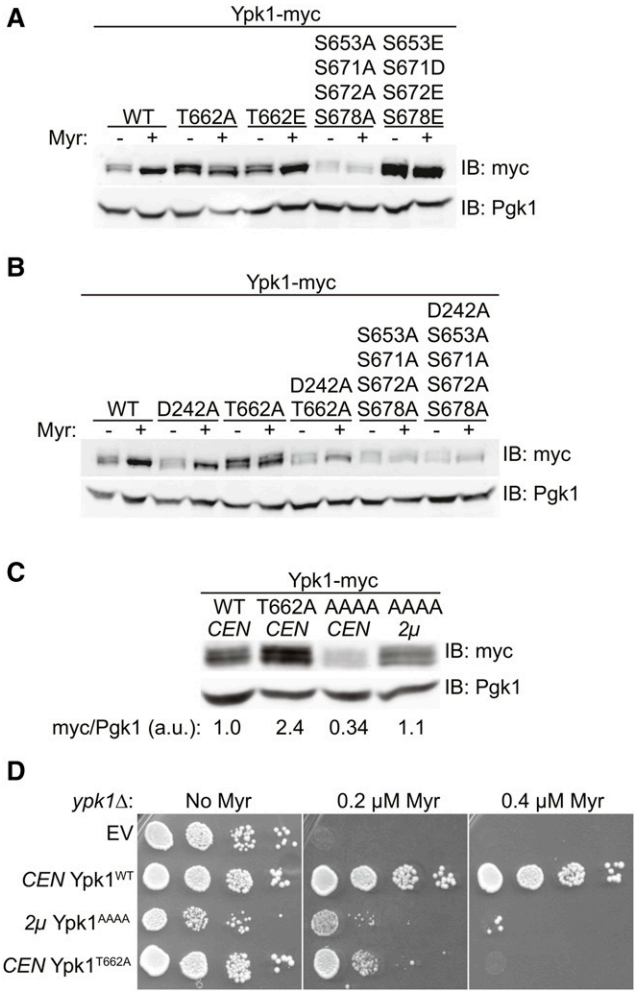

Figure 5 Phosphorylation at the new C-terminal sites promotes Ypk1 stability. (A) Cultures of *ypk1*Δ cells containing empty vector (pRS315) or the same plasmid expressing Ypk1^{WT}-myc (pAM20), Ypk1^{T662A}-myc (pFR221), Ypk1^{T662E}-myc (pFR284), Ypk1$^{S653A\ S671A\ S672A\ S678A}$-myc (pJEN3), or Ypk1$^{S653E\ S671D\ S672E\ S678E}$-myc (pJEN6) were grown to midexponential phase and then treated with vehicle (methanol) or 1.25 μM Myr for 2 hr. After harvesting, whole-cell lysates were prepared, resolved by SDS-PAGE, and analyzed by immunoblotting with anti-myc mAb 9E10. (B) Cultures of *ypk1*Δ cells containing empty vector (pRS315) or the same plasmid expressing Ypk1^{WT}-myc (pAM20), Ypk1^{D242A}-myc (pFR234), Ypk1^{T662A}-myc (pFR221), Ypk1$^{D242A\ T662A}$-myc (pKL7), Ypk1$^{S653A\ S671A\ S672A\ S678A}$-myc (pJEN3), or Ypk1$^{D242A\ S653A\ S671A\ S672A\ S678A}$-myc (pJEN4) were treated and analyzed as in (A). (C) Cultures of *ypk1*Δ cells expressing from a *CEN* plasmid either Ypk1^{WT}-myc (pAM20), Ypk1^{T662A}-myc (pFR221), or Ypk1$^{S653A\ S671A\ S672A\ S678A}$-myc (pJEN3), or expressing from a 2 μm DNA plasmid Ypk1$^{S653A\ S671A\ S672A\ S678A}$-myc (pKL49), as indicated, were grown to midexponential phase, harvested, and analyzed as in (A). (D) Cultures of *ypk1*Δ cells containing empty vector (EV) (pRS315), a *CEN* plasmid expressing Ypk1^{WT}-myc (pAM20), a 2 *μm* DNA plasmid expressing Ypk1$^{S653A\ S671A\ S672A\ S678A}$-myc (pKL49), or a *CEN* plasmid expressing Ypk1^{T662A}-myc (pFR221) were adjusted to a cell density of $A_{600\ nm}$ = 1.0 and then spotted in 10-fold serial dilutions onto SCD-Leu agar plates containing vehicle (methanol) or the indicated concentration of Myr. Plates were then incubated at 30° for 2 days prior to imaging. IB, immunoblot.

sites in both the turn and hydrophobic motifs was unaffected, *i.e.*, comparable to that in Ypk1^{WT}-3HA (Figure 6B). These results show, first, that the modifications at Thr504 and Thr662 occur independently of each other. Second, and more importantly, these findings indicate that the multiple TORC2-mediated modifications at the C-terminal sites (namely at Ser653, Ser671, Ser672, and Ser678) are a prelude to and prerequisite for efficient TORC2-dependent modification of Thr662 (and, presumably, Ser644).

Discussion

Like all eukaryotic protein kinases, members of the AGC subfamily of these enzymes share a common catalytic domain structure consisting of a small N-terminal lobe (N-lobe) and larger C-terminal lobe (C-lobe) with the active site sandwiched between the N-lobe and C-lobe (Pearce *et al.* 2010). In AGC-family kinases, phosphorylation at several conserved sites is necessary for their catalytic function. A conserved site essential for activity resides in the activation loop, which is situated nearby the ATP-binding site in the kinase domain. The activation loop, when phosphorylated, makes vital contacts with the catalytic loop and the αC helix; the cumulative conformational changes so induced are essential for opening up the active site cleft, for positioning the catalytic Asp in the proper location, and for enhancing contacts with ATP in its binding pocket, all of which are necessary for catalytic activity (Yang *et al.* 2002b; Komander *et al.* 2005). A second conserved phosphorylation site is the hydrophobic motif near the C terminus. In the structure of mammalian AKT/PKB, the C-terminal sequence extends from the C-lobe, wraps around the N-lobe, and fits into a hydrophobic groove comprised, in part, by the αC helix (Yang *et al.* 2002a,b). When phosphorylated, the hydrophobic motif appears to stabilize the αC helix in the conformation found in the active state of AKT (Yang *et al.* 2002a,b). AKT and other AGC-family protein kinases (*e.g.*, S6K, RSK, MSK, PRK, and PKCs) have a third conserved site, known as the turn motif, located in the C-terminal tail upstream of the hydrophobic motif. When phosphorylated, the turn motif interacts with a positively charged pocket in the N-lobe and further stabilizes wrapping of the C-terminal tail around the N-lobe (Grodsky *et al.* 2006; Hauge *et al.* 2007). Thus, phosphorylations at the hydrophobic motif and turn motif buttress the active state of an AGC kinase and are necessary for its full activation.

On the basis of both sequence homology and organization, Ypk1 is clearly a member of the AGC family of protein kinases (Casamayor *et al.* 1999; Roelants *et al.* 2004). Moreover, Ypk1 is known to require phosphorylation at its activation loop (Thr504) and to be regulated by phosphorylation at its hydrophobic motif (Thr662). Phosphorylation at Thr504 in the activation loop catalyzed by Pkh1 (and Pkh2), which is essential for basal Ypk1 activity (Roelants *et al.* 2004), does not change in response to the stress of sphingolipid depletion (Roelants *et al.* 2010), but purportedly increases in response to heat stress (Omnus *et al.* 2016). TORC2 mediates hydrophobic motif phosphorylation (Roelants *et al.* 2011), which is markedly stimulated by sphingolipid depletion (Roelants *et al.* 2011; Berchtold *et al.* 2012), hypotonic conditions

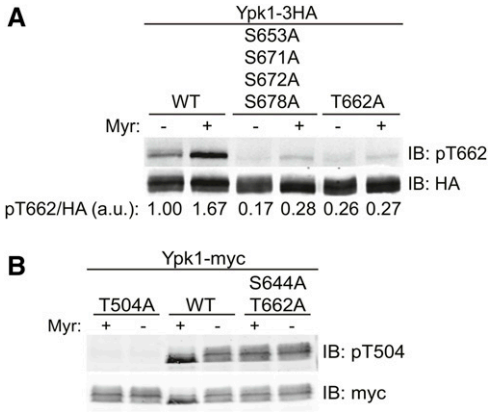

Figure 6 Phosphorylation of the new C-terminal sites is necessary for efficient hydrophobic motif phosphorylation. (A) Cultures of *ypk1*Δ cells containing plasmids expressing Ypk1-3HA (pPL215), Ypk1$^{S653A\ S671A\ S672A\ S678A}$-3HA (pJEN5), or Ypk1^{T662A}-3HA (pKL32) were grown to midexponential phase in SCD-Ura then treated with either vehicle (methanol) or 1.25 μM Myr for 2 hr, as indicated. After harvesting, whole-cell extracts were prepared, resolved by SDS-PAGE, and analyzed by immunoblotting with anti-HA and anti-phosphoT662 Ypk1 antibodies. The volume of extract loaded in each lane was adjusted to ensure that the total amount of each Ypk1 variant was equivalent. (B) Strain BY4741 (*YPK1*$^+$) containing plasmids expressing from the *GAL* promoter Ypk1^{T504A}-myc (pFR111), Ypk1^{WT}-myc (pAM76), or Ypk1$^{S644A\ T662A}$-myc (pFR112) were treated with vehicle (methanol) or 1.25 μM Myr for 2 hr and then analyzed by SDS-PAGE and immunoblotting as in (A), except that the antibodies used were anti-myc mAb 9E10 and anti-phospho-Thr256 SGK1 antibodies.

(Berchtold *et al.* 2012), heat shock (Sun *et al.* 2012), and acetic acid stress (Guerreiro *et al.* 2016).

As we have confirmed here, the turn motif in Ypk1 (Roelants *et al.* 2004) is also essential for Ypk1 function. Moreover, as documented here, we discovered that TORC2 also phosphorylates four other C-terminal sites in Ypk1 (Ser653, Ser671, Ser672, and Ser678) that lie in close propinquity to the turn and hydrophobic motifs. Although we demonstrated that purified Ypk1 is a substrate for purified TORC2 *in vitro*, we have not shown that the residues in Ypk1 subject to TORC2-mediated phosphorylation include these four new sites. It remains, therefore, a formal possibility that, in the cell, phosphorylation at one or more of these positions is mediated by a TORC2-dependent protein kinase rather than TORC2 itself. However, because TORC2 was the only Ser/Thr kinase that, when inactivated, abolished phosphorylation at these residues *in vivo*, they are very likely direct phosphoacceptor sites for TORC2. Consistent with that conclusion, the minimal consensus shared among the turn and hydrophobic motifs and the new sites is -S/T-Hpo-, where Hpo designates any hydrophobic residue bulkier than Ala. It is worth noting in this same regard that several other phosphorylation sites identified in our MS experiments also have a bulky hydrophobic residue at the +1 position, and phosphorylation at some of these sites (*e.g.*, Thr57) was elevated after Myr treatment (data not shown). Although lack of phosphorylation at these sites did not cause any mobility shift on Phos-tag gels that we could monitor, we have not ruled out the possibility that these phosphorylation sites may nonetheless be under TORC2 control and/or direct targets of TORC2.

In any event, we have demonstrated here that TORC2-mediated phosphorylation at S653, S671, S672, and S678 is necessary for full Ypk1 function. Taken together, the most parsimonious interpretation of our data is that TORC2 phosphorylates its preferred sites at the C terminus of Ypk1, perhaps sequentially, starting from the C terminus. Presumably, successive modification helps destabilize and peel back the C-terminal segment of the protein, making the next site more accessible, allowing TORC2 readier access to the hydrophobic motif and the turn motif, which, once modified, can then bind to and lock in the active conformation of the N-lobe of the kinase fold. In this way, phosphorylation of the four new sites allows for optimal phosphorylation of Ypk1 at its hydrophobic and turn motif, consistent with our finding that preventing phosphorylation of Ypk1 at the four C-terminal sites makes cells Myr sensitive and prevents hydrophobic motif phosphorylation. Likewise, loss of three of these sites (S653, S671, and S672) was also sufficient to confer Myr sensitivity and compromise Thr662 phosphorylation (data not shown), whereas retention of phosphorylation at even two of these sites permitted Ypk1 function. Several additional findings reinforce the conclusion that these new C-terminal sites are physiologically important. In our MS analysis, when cells were treated with Myr, in addition to elevation of S644 and T662 phosphorylation, we found a readily detectable increase in phosphorylation at the most proximal site (S653) (data not shown). In agreement with our observations, in a very recent global phosphoproteomics study, increased phosphorylation of Ypk1 at both S653 and S672 were observed following Myr treatment (Lebesgue *et al.* 2017). Thus, it does appear that TORC2 responds to sphingolipid depletion by enhancing phosphorylation of Ypk1 at the four C-terminal sites, which, in turn, allows for efficient hydrophobic and turn motif phosphorylation. In a similar way, it has been reported that, in response to the stress of a nonphysiological concentration (10 mM) of exogenous methylglyoxal, phosphorylation of Pkc1, another AGC kinase in *S. cerevisiae* that is a target of TORC2 (Ho *et al.* 2005; Kamada *et al.* 2005), is increased at sites corresponding to its turn and hydrophobic motifs (Roelants *et al.* 2004; Nomura and Inoue 2015). Moreover, lack of phosphorylation at the turn motif site (T1125 in Pkc1) reduces the efficiency of phosphorylation at the hydrophobic motif (S1143 in Pkc1) and vice versa (Nomura and Inoue 2015), reminiscent of the interdependencies we found for phosphorylation among the C-terminal sites in Ypk1.

Modification of Ser644 in the turn motif is presumed to be under the control of TORC2. Indeed, in our MS study, we found an increase in Ser644 phosphorylation after Myr treatment (data not shown). Moreover, a Ypk1^{S644A}-myc mutant was inviable even at the lowest concentrations of Myr tested and was even more sensitive to Myr than a Ypk1^{T662A}-myc mutant. Thus, S644 phosphorylation is critical for Ypk1 function (although we could not readily monitor S644 phosphorylation by immunoblotting because, currently, a phospho-site-specific antibody that reliably

reports this modification in Ypk1 is not available). Quite similarly, phosphorylation at the turn motif *per se* has been reported to be important for proper C-terminal folding and stability of mammalian AKT and PKC (Facchinetti *et al.* 2008; Ikenoue *et al.* 2008). In this regard, we also found that absence of phosphorylation at the four new C-terminal phosphorylation sites diminished the steady-state level of Ypk1 significantly, in further agreement with the model that TORC2-mediated phosphorylation at the four C-terminal sites promotes modification of Ser644 and the function of that modification is stabilizing Ypk1, as it does in the mammalian AGC kinases. In any event, collectively, our observations document that full TORC2-dependent phosphorylation of Ypk1 at six C-terminal sites (the four new sites and the turn and hydrophobic motifs) is necessary for optimal Ypk1 function.

To date, there is no available crystal or NMR structure for Ypk1. There is a reported crystal structure at 1.9-Å resolution for a 431-residue splice variant of SGK1, the human ortholog of Ypk1 (Casamayor *et al.* 1999), in a complex with an Mg^{2+}-bound, nonhydrolyzable ATP analog (AMPPNP); however, in this structure, 59 N-terminal residues were deleted and 6 substitution mutations (S74A S78A R192A S397A S401A S422D) were introduced to "stabilize" the protein (Zhao *et al.* 2007). Overall, the structure obtained most closely resembles the inactive conformations of other AGC kinases and the αC helix is totally absent (because it adopts, instead, a β-strand arrangement via formation of an antiparallel β-sheet with a portion of the sequence corresponding to the activation loop). Thus, the construct analyzed is of little utility for understanding authentic SGK1 function.

Ypk1 contains a well-conserved kinase domain and a prominent N-terminal extension that is four times larger than its C-terminal extension. The exact function of the Ypk1 N-terminal domain is unknown, but several observations indicate that it serves a negative regulatory role. First, unlike overexpression of full-length Ypk1, overexpressing an N-terminally truncated Ypk1ΔN mutant is toxic to cells, whereas overexpressing a kinase-dead derivative of the Ypk1ΔN mutant is not (Roelants *et al.* 2002). Second, as we showed before, a Ypk1 mutant with an N-terminal substitution mutation (D242A) rescues the inviability of a *tor2*^{ts} allele (Roelants *et al.* 2011), suggesting that alteration of the N-terminal domain alleviates the need for TORC2-dependent phosphorylation of Ypk1. Third, we confirmed and solidified that conclusion by documenting here that the D242A mutation suppresses the loss-of-function phenotypes of Ypk1 mutants that cannot be phosphorylated at the hydrophobic motif, at the turn motif, and at all four of the new C-terminal sites. The simplest model to explain how the D242A point mutation bypasses the need for TORC2 phosphorylation is that, normally, the N-terminal domain interacts with and constrains the kinase fold in an inactive conformation and the role of the C terminus is to compete with and displace this N-terminal inhibitory domain, which the C terminus can only do effectively when it is phosphorylated. In the D242A mutant, the inhibitory role of the N-terminal domain is presumably crippled, allowing the kinase fold to more easily adopt its active conformation, even in the absence of TORC2-dependent phosphorylation of the C-terminal sites. A purely speculative model for how the negatively charged Asp242 residue in the N-terminal regulatory domain might exert its negative influence and compete with TORC2-mediated phosphorylation of the C-terminal sites is by specifically occupying a binding pocket lined with basic residues which can only be bound by the turn motif when it is phosphorylated, equivalent to the interaction revealed in the crystal structures of the activated states of several mammalian AGC kinase family members (Grodsky *et al.* 2006; Hauge *et al.* 2007). Thus, when such a critical D242-dependent salt bridge(s) is broken by mutation to Ala, the inhibitory constraint imposed by the N-terminal negative regulatory domain is relieved without the need for any competitive binding by phosphorylated C-terminal sites. Indeed, consistent with this speculative model, in otherwise WT Ypk1, mutation of either the four new C-terminal sites to Glu/Asp or the hydrophobic motif to Glu was sufficient to maintain full biological function, indicating that the presence of negatively charged residues in this region is sufficient to outcompete and overcome the inhibitory effect of the N-terminal domain. However, Ypk1^{D242A} itself is clearly not hyperactive; stimulation of its TORC2-dependent phosphorylation by Myr treatment markedly increased Ypk1-mediated phosphorylation of an *in vivo* target (Orm1). Thus, negative charges at the C-terminal end (either authentic phosphate groups or a negatively charged amino acid side chain) are still needed, presumably to maximize interaction with and optimally stabilize the kinase domain in its active conformation, again akin to what is observed in the crystal structures of the activated state of AKT (Yang *et al.* 2002a,b) and other mammalian AGC kinases (Grodsky *et al.* 2006; Hauge *et al.* 2007). Indeed, mammalian AKT is phosphorylated in an mTORC2-dependent manner at C-terminal sites in addition to its turn and hydrophobic motifs (Liu *et al.* 2014). Moreover, consistent with what we have observed for Ypk1, phosphorylation of AKT at its C terminus is necessary for efficient hydrophobic motif phosphorylation (Liu *et al.* 2014).

S. cerevisiae encodes a functional Ypk1 paralog, Ypk2 (Chen *et al.* 1993; Roelants *et al.* 2002). Reassuringly, in global phospho-proteomic studies (Holt *et al.* 2009; Swaney *et al.* 2013), sites of phosphorylation in Ypk2 have been reported that correspond to S653 and S672 in Ypk1, suggesting that Ypk2 is likely regulated by TORC2 in a manner similar to Ypk1. Moreover, a site equivalent to S678 in Ypk1 is also conserved in Ypk2. The only exception is that the residue corresponding to S671 in Ypk1 is already a negatively charged residue (Asp) in Ypk2 and is not conserved in three of the more distant Ypk1 orthologs, indicating that in all these enzymes the residue equivalent to S672 in Ypk1 is the important site for TORC2-dependent phosphorylation at this location. Interestingly, the residue in Ypk2 that corresponds to Ser672 in Ypk1 is followed by Pro, suggesting that Pro is among the hydrophobic residues that TORC2 is able to recognize at the position +1 to the phospho-acceptor residue. In *S. cerevisiae*, Sch9, another

AGC-family protein kinase, is phosphorylated by TORC1 at multiple C-terminal positions in addition to the sites equivalent to its turn and hydrophobic motifs (Urban *et al.* 2007). Just as we have shown here for TORC2-mediated phosphorylation of Ypk1, TORC1-mediated phosphorylation of Sch9 at these novel C-terminal sites also changes in response to stresses that are known to modulate TORC1 activity, such as carbon and nitrogen starvation (Urban *et al.* 2007). Also, as with the new C-terminal sites we characterized in Ypk1, the TORC1 phosphorylation sites in Sch9 exhibit a preference for a hydrophobic (alkyl or aromatic) residue at the position +1 to the phospho-acceptor residue (Urban *et al.* 2007), which may explain why either Tor1 or Tor2 can function in TORC1. Similarly, it has been reported that mTOR also prefers a hydrophobic (alkyl, including Pro, or aromatic) residue in the +1 position (Hsu *et al.* 2011). In conclusion, our detailed analysis of yeast Ypk1 demonstrates that extensive C-terminal phosphorylation is a conserved mechanism by which TOR complexes regulate AGC-family protein kinases.

Acknowledgments

We acknowledge assistance with the mass spectrometry analysis of Ypk1-derived phospho-peptides provided by David Breslow (University of California, San Francisco; now at Yale University) and Bernd Bodenmiller (Stanford University; now at University of Zürich, Switzerland). We also thank Ted Powers (University of California, Davis) for the generous gift of anti-phospho-T662 Ypk1 antibodies and certain plasmids, and the staff of the University of California Berkeley DNA Sequencing Facility for verification of all of the constructs used in this study. This work was supported by National Institutes of Health predoctoral traineeship GM-07232 (to K.L.L.) and by National Institutes of Health research grant R01 GM-21841 (to J.T.).

Literature Cited

Alvaro, C. G., A. Aindow, and J. Thorner, 2016 Differential phosphorylation provides a switch to control how α-arrestin Rod1 down-regulates mating pheromone response in *Saccharomyces cerevisiae*. Genetics 203: 299–317.

Aylett, C. H., E. Sauer, S. Imseng, D. Boehringer, M. N. Hall *et al.*, 2016 Architecture of human mTOR complex 1. Science 351: 48–52.

Baretić, D., A. Berndt, Y. Ohashi, C. M. Johnson, and R. L. Williams, 2016 Tor forms a dimer through an N-terminal helical solenoid with a complex topology. Nat. Commun. 7: 11016.

Bartlett, K., and K. Kim, 2014 Insight into Tor2, a budding yeast microdomain protein. Eur. J. Cell Biol. 93: 87–97.

Benton, B. M., J. H. Zang, and J. Thorner, 1994 A novel FK506- and rapamycin-binding protein (*FPR3* gene product) in the yeast *Saccharomyces cerevisiae* is a proline rotamase localized to the nucleolus. J. Cell Biol. 127: 623–639.

Berchtold, D., and T. C. Walther, 2009 TORC2 plasma membrane localization is essential for cell viability and restricted to a distinct domain. Mol. Biol. Cell 20: 1565–1575.

Berchtold, D., M. Piccolis, N. Chiaruttini, I. Riezman, H. Riezman *et al.*, 2012 Plasma membrane stress induces relocalization of Slm proteins and activation of TORC2 to promote sphingolipid synthesis. Nat. Cell Biol. 14: 542–547.

Betz, C., and M. N. Hall, 2013 Where is mTOR and what is it doing there? J. Cell Biol. 203: 563–574.

Breslow, D. K., S. R. Collins, B. Bodenmiller, R. Aebersold, K. Simons *et al.*, 2010 Orm family proteins mediate sphingolipid homeostasis. Nature 463: 1048–1053.

Casamayor, A., P. D. Torrance, T. Kobayashi, J. Thorner, and D. R. Alessi, 1999 Functional counterparts of mammalian protein kinases PDK1 and SGK in budding yeast. Curr. Biol. 9: 186–197.

Chen, P., K. S. Lee, and D. E. Levin, 1993 A pair of putative protein kinase genes (*YPK1* and *YPK2*) is required for cell growth in *Saccharomyces cerevisiae*. Mol. Gen. Genet. 236: 443–447.

Cliften, P., P. Sudarsanam, A. Desikan, L. Fulton, B. Fulton *et al.*, 2003 Finding functional features in Saccharomyces genomes by phylogenetic footprinting. Science 301: 71–76.

Costanzo, M., A. Baryshnikova, J. Bellay, Y. Kim, E. D. Spear *et al.*, 2010 The genetic landscape of a cell. Science 327: 425–431.

Dickson, R. C., C. Sumanasekera, and R. L. Lester, 2006 Functions and metabolism of sphingolipids in *Saccharomyces cerevisiae*. Prog. Lipid Res. 45: 447–465.

Divito, C. B., and S. G. Amara, 2009 Close encounters of the oily kind: regulation of transporters by lipids. Mol. Interv. 9: 252–262.

Dunn, T. M., D. V. Lynch, L. V. Michaelson, and J. A. Napier, 2004 A post-genomic approach to understanding sphingolipid metabolism in *Arabidopsis thaliana*. Ann. Bot. 93: 483–497.

Eltschinger, S., and R. Loewith, 2016 TOR complexes and the maintenance of cellular homeostasis. Trends Cell Biol. 26: 148–159.

Facchinetti, V., W. Ouyang, H. Wei, N. Soto, A. Lazorchak *et al.*, 2008 The mammalian target of rapamycin complex 2 controls folding and stability of Akt and protein kinase C. EMBO J. 27: 1932–1943.

Fröhlich, F., D. K. Olson, R. Christiano, R. V. J. Farese, and T. C. Walther, 2016 Proteomic and phosphoproteomic analyses of yeast reveal the global cellular response to sphingolipid depletion. Proteomics 16: 2759–2763.

Gaubitz, C., T. M. Oliveira, M. Prouteau, A. Leitner, M. Karuppasamy *et al.*, 2015 Molecular basis of the rapamycin insensitivity of target of Rapamycin Complex 2. Mol. Cell 58: 977–988.

Gaubitz, C., M. Prouteau, B. Kusmider, and R. Loewith, 2016 TORC2 structure and function. Trends Biochem. Sci. 41: 532–545.

Gelperin, D. M., M. A. White, M. L. Wilkinson, Y. Kon, L. A. Kung *et al.*, 2005 Biochemical and genetic analysis of the yeast proteome with a movable ORF collection. Genes Dev. 19: 2816–2826.

Grodsky, N., Y. Li, D. Bouzida, R. Love, J. Jensen *et al.*, 2006 Structure of the catalytic domain of human protein kinase C beta II complexed with a bisindolylmaleimide inhibitor. Biochemistry 45: 13970–13981.

Groves, J. T., and J. Kuriyan, 2010 Molecular mechanisms in signal transduction at the membrane. Nat. Struct. Mol. Biol. 17: 659–665.

Guerreiro, J. F., A. Muir, S. Ramachandran, J. Thorner, and I. Sá-Correia, 2016 Sphingolipid biosynthesis upregulation by TOR Complex 2-Ypk1 signaling during yeast adaptive response to acetic acid stress. Biochem. J. 473: 4311–4325.

Hauge, C., T. L. Antal, D. Hirschberg, U. Doehn, K. Thorup *et al.*, 2007 Mechanism for activation of the growth factor-activated AGC kinases by turn motif phosphorylation. EMBO J. 26: 2251–2261.

Heitman, J., N. R. Movva, and M. N. Hall, 1991 Targets for cell cycle arrest by the immunosuppressant rapamycin in yeast. Science 253: 905–909.

Helliwell, S. B., P. Wagner, J. Kunz, M. Deuter-Reinhard, R. Henriquez *et al.*, 1994 TOR1 and TOR2 are structurally and functionally similar but not identical phosphatidylinositol kinase homologues in yeast. Mol. Biol. Cell 5: 105–118.

Helliwell, S. B., I. Howald, N. Barbet, and M. N. Hall, 1998 TOR2 is part of two related signaling pathways coordinating cell growth in Saccharomyces cerevisiae. Genetics 148: 99–112.

Hill, J. E., A. M. Myers, T. J. Koerner, and A. Tzagoloff, 1986 Yeast/E. coli shuttle vectors with multiple unique restriction sites. Yeast 2: 163–167.

Ho, H. L., Y. S. Shiau, and M. Y. Chen, 2005 *Saccharomyces cerevisiae* TSC11/AVO3 participates in regulating cell integrity and functionally interacts with components of the Tor2 complex. Curr. Genet. 47: 273–288.

Holt, L. J., B. B. Tuch, J. Villén, A. D. Johnson, S. P. Gygi *et al.*, 2009 Global analysis of Cdk1 substrate phosphorylation sites provides insights into evolution. Science 325: 1682–1686.

Hsu, P. P., S. A. Kang, J. Rameseder, Y. Zhang, K. A. Ottina *et al.*, 2011 The mTOR-regulated phosphoproteome reveals a mechanism of mTORC1-mediated inhibition of growth factor signaling. Science 332: 1317–1322.

Huang, J., and B. D. Manning, 2009 A complex interplay between Akt, TSC2 and the two mTOR complexes. Biochem. Soc. Trans. 37: 217–222.

Huber, A., B. Bodenmiller, A. Uotila, M. Stahl, S. Wanka *et al.*, 2009 Characterization of the rapamycin-sensitive phosphoproteome reveals that Sch9 is a central coordinator of protein synthesis. Genes Dev. 23: 1929–1943.

Ikai, N., N. Nakazawa, T. Hayashi, and M. Yanagida, 2011 The reverse, but coordinated, roles of Tor2 (TORC1) and Tor1 (TORC2) kinases for growth, cell cycle and separase-mediated mitosis in *Schizosaccharomyces pombe*. Open Biol. 1: 110007.

Ikenoue, T., K. Inoki, Q. Yang, X. Zhou, and K. L. Guan, 2008 Essential function of TORC2 in PKC and Akt turn motif phosphorylation, maturation and signalling. EMBO J. 27: 1919–1931.

Ikushiro, H., H. Hayashi, and H. Kagamiyama, 2004 Reactions of serine palmitoyltransferase with serine and molecular mechanisms of the actions of serine derivatives as inhibitors. Biochemistry 43: 1082–1092.

Jacinto, E., R. Loewith, A. Schmidt, S. Lin, M. A. Rüegg *et al.*, 2004 Mammalian TOR complex 2 controls the actin cytoskeleton and is rapamycin insensitive. Nat. Cell Biol. 6: 1122–1128.

Kamada, Y., Y. Fujioka, N. N. Suzuki, F. Inagaki, S. Wullschleger *et al.*, 2005 Tor2 directly phosphorylates the AGC kinase Ypk2 to regulate actin polarization. Mol. Cell. Biol. 25: 7239–7248.

Kellis, M., N. Patterson, M. Endrizzi, B. Birren, and E. S. Lander, 2003 Sequencing and comparison of yeast species to identify genes and regulatory elements. Nature 423: 241–254.

Kinoshita, E., E. Kinoshita-Kikuta, and T. Koike, 2015 Advances in Phos-tag-based methodologies for separation and detection of the phosphoproteome. Biochim. Biophys. Acta 1854: 601–608.

Kliegman, J. I., D. Fiedler, C. J. Ryan, Y. F. Xu, X. Y. Su *et al.*, 2013 Chemical genetics of rapamycin-insensitive TORC2 in S. cerevisiae. Cell Rep. 5: 1725–1736.

Komander, D., G. Kular, M. Deak, D. R. Alessi, and D. M. van Aalten, 2005 Role of T-loop phosphorylation in PDK1 activation, stability, and substrate binding. J. Biol. Chem. 280: 18797–18802.

Kunz, J., R. Henriquez, U. Schneider, M. Deuter-Reinhard, N. R. Movva *et al.*, 1993 Target of rapamycin in yeast, TOR2, is an essential phosphatidylinositol kinase homolog required for G1 progression. Cell 73: 585–596.

Kunz, J., U. Schneider, I. Howald, A. Schmidt, and M. N. Hall, 2000 HEAT repeats mediate plasma membrane localization of Tor2p in yeast. J. Biol. Chem. 275: 37011–37020.

Lebesgue, N., M. Megyeri, A. Cristobal, A. Scholten, G. G. Chuartzman *et al.*, 2017 Combining deep sequencing, proteomics, phosphoproteomics, and functional screens to discover novel regulators of sphingolipid homeostasis. J. Proteome Res. 16: 571–582.

Lee, Y. J., G. R. Jeschke, F. M. Roelants, J. Thorner, and B. E. Turk, 2012 Reciprocal phosphorylation of yeast glycerol-3-phosphate dehydrogenases in adaptation to distinct types of stress. Mol. Cell. Biol. 32: 4705–4717.

Liu, P., M. Begley, W. Michowski, H. Inuzuka, M. Ginzberg *et al.*, 2014 Cell-cycle-regulated activation of Akt kinase by phosphorylation at its carboxyl terminus. Nature 508: 541–545.

Loewith, R., and M. N. Hall, 2011 Target of rapamycin (TOR) in nutrient signaling and growth control. Genetics 189: 1177–1201.

Loewith, R., E. Jacinto, S. Wullschleger, A. Lorberg, J. L. Crespo *et al.*, 2002 Two TOR complexes, only one of which is rapamycin sensitive, have distinct roles in cell growth control. Mol. Cell 10: 457–468.

Megyeri, M., H. Riezman, M. Schuldiner, and A. H. Futerman, 2016 Making sense of the yeast sphingolipid pathway. J. Mol. Biol. 428: 4765–4775.

Miyake, Y., Y. Kozutsumi, S. Nakamura, T. Fujita, and T. Kawasaki, 1995 Serine palmitoyl-transferase is the primary target of a sphingosine-like immunosuppressant, ISP-1/myriocin. Biochem. Biophys. Res. Commun. 211: 396–403.

Mok, J., P. M. Kim, H. Y. Lam, S. Piccirillo, X. Zhou *et al.*, 2010 Deciphering protein kinase specificity through large-scale analysis of yeast phosphorylation site motifs. Sci. Signal. 3: ra12.

Momoi, M., D. Tanoue, Y. Sun, H. Takematsu, Y. Suzuki *et al.*, 2004 SLI1 (YGR212W) is a major gene conferring resistance to the sphingolipid biosynthesis inhibitor ISP-1, and encodes an ISP-1 N-acetyltransferase in yeast. Biochem. J. 381: 321–328.

Muir, A., S. Ramachandran, F. M. Roelants, G. Timmons, and J. Thorner, 2014 TORC2-dependent protein kinase Ypk1 phosphorylates ceramide synthase to stimulate synthesis of complex sphingolipids. Elife 3: e03779.

Muir, A., F. M. Roelants, G. Timmons, K. L. Leskoske, and J. Thorner, 2015 Down-regulation of TORC2-Ypk1 signaling promotes MAPK-independent survival under hyperosmotic stress. Elife 4: e09336.

Niles, B. J., H. Mogri, A. Hill, A. Vlahakis, and T. Powers, 2012 Plasma membrane recruitment and activation of the AGC kinase Ypk1 is mediated by target of rapamycin complex 2 (TORC2) and its effector proteins Slm1 and Slm2. Proc. Natl. Acad. Sci. USA 109: 1536–1541.

Nomura, W., and Y. Inoue, 2015 Methylglyoxal activates the target of rapamycin complex 2-protein kinase C signaling pathway in *Saccharomyces cerevisiae*. Mol. Cell. Biol. 35: 1269–1280.

Olson, D. K., F. Fröhlich, R. V. Farese, and T. C. Walther, 2016 Taming the sphinx: mechanisms of cellular sphingolipid homeostasis. Biochim. Biophys. Acta 1861: 784–792.

Omnus, D. J., A. G. Manford, J. M. Bader, S. D. Emr, and C. J. Stefan, 2016 Phosphoinositide kinase signaling controls ER-PM cross-talk. Mol. Biol. Cell 27: 1170–1180.

Pearce, L. R., D. Komander, and D. R. Alessi, 2010 The nuts and bolts of AGC protein kinases. Nat. Rev. Mol. Cell Biol. 11: 9–22.

Platta, H. W., and H. Stenmark, 2011 Endocytosis and signaling. Curr. Opin. Cell Biol. 23: 393–403.

Roelants, F. M., P. D. Torrance, N. Bezman, and J. Thorner, 2002 Pkh1 and Pkh2 differentially phosphorylate and activate Ypk1 and Ykr2 and define protein kinase modules required for maintenance of cell wall integrity. Mol. Biol. Cell 13: 3005–3028.

Roelants, F. M., P. D. Torrance, and J. Thorner, 2004 Differential roles of PDK1- and PDK2-phosphorylation sites in the yeast AGC kinases Ypk1, Pkc1 and Sch9. Microbiology 150: 3289–3304.

Roelants, F. M., A. G. Baltz, A. E. Trott, S. Fereres, and J. Thorner, 2010 A protein kinase network regulates the function of aminophospholipid flippases. Proc. Natl. Acad. Sci. USA 107: 34–39.

Roelants, F. M., D. K. Breslow, A. Muir, J. S. Weissman, and J. Thorner, 2011 Protein kinase Ypk1 phosphorylates regulatory proteins Orm1 and Orm2 to control sphingolipid homeostasis in Saccharomyces cerevisiae. Proc. Natl. Acad. Sci. USA 108: 19222–19227.

Roelants, F. M., K. L. Leskoske, R. T. Pedersen, A. Muir, J. M. Liu *et al.*, 2017 TOR Complex 2-regulated protein kinase Fpk1 stimulates endocytosis via inhibition of Ark1/Prk1-related protein kinase Akl1 in *Saccharomyces cerevisiae*. Mol. Cell. Biol. 37: e00627-16.

Rubenstein, E. M., and M. C. Schmidt, 2007 Mechanisms regulating the protein kinases of *Saccharomyces cerevisiae*. Eukaryot. Cell 6: 571–583.

Sambrook, J., E. F. Fritsh, and T. Maniatis, 1989 *Molecular Cloning: A Laboratory Manual*. Cold Spring Harbor Lab Press, Cold Spring Harbor, NY.

Sherman, F., G. R. Fink, and J. B. Hicks, 1986 *Laboratory Course Manual for Methods in Yeast Genetics*. Cold Spring Harbor Lab Press, Cold Spring Harbor, NY.

Sikorski, R. S., and P. Hieter, 1989 A system of shuttle vectors and yeast host strains designed for efficient manipulation of DNA in Saccharomyces cerevisiae. Genetics 122: 19–27.

Simons, K., and J. L. Sampaio, 2011 Membrane organization and lipid rafts. Cold Spring Harb. Perspect. Biol. 3: a004697.

Sun, Y., Y. Miao, Y. Yamane, C. Zhang, K. M. Shokat *et al.*, 2012 Orm protein phospho-regulation mediates transient sphingolipid biosynthesis response to heat stress via the Pkh-Ypk and Cdc55–PP2A pathways. Mol. Biol. Cell 23: 2388–2398.

Swaney, D. L., P. Beltrao, L. Starita, A. Guo, J. Rush *et al.*, 2013 Global analysis of phosphorylation and ubiquitylation cross-talk in protein degradation. Nat. Methods 10: 676–682.

Tanoue, D., T. Kobayashi, Y. Sun, T. Fujita, H. Takematsu *et al.*, 2005 The requirement for the hydrophobic motif phosphorylation of Ypk1 in yeast differs depending on the downstream events, including endocytosis, cell growth, and resistance to a sphingolipid biosynthesis inhibitor, ISP-1. Arch. Biochem. Biophys. 437: 29–41.

Urban, J., A. Soulard, A. Huber, S. Lippman, D. Mukhopadhyay *et al.*, 2007 Sch9 is a major target of TORC1 in Saccharomyces cerevisiae. Mol. Cell 26: 663–674.

Wedaman, K. P., A. Reinke, S. Anderson, and J. Yates, IIIJ. M. McCaffery *et al.*, 2003 Tor kinases are in distinct membrane-associated protein complexes in Saccharomyces cerevisiae. Mol. Biol. Cell 14: 1204–1220.

Yang, H., D. G. Rudge, J. D. Koos, B. Vaidialingam, H. J. Yang *et al.*, 2013 mTOR kinase structure, mechanism and regulation. Nature 497: 217–223.

Yang, J., P. Cron, V. M. Good, V. Thompson, B. A. Hemmings *et al.*, 2002a Crystal structure of an activated Akt/protein kinase B ternary complex with GSK3-peptide and AMP-PNP. Nat. Struct. Biol. 9: 940–944.

Yang, J., P. Cron, V. Thompson, V. M. Good, D. Hess *et al.*, 2002b Molecular mechanism for the regulation of protein kinase B/Akt by hydrophobic motif phosphorylation. Mol. Cell 9: 1227–1240.

Yeung, B. K., 2011 Natural product drug discovery: the successful optimization of ISP-1 and halichondrin B. Curr. Opin. Chem. Biol. 15: 523–528.

Zhao, B., R. Lehr, A. M. Smallwood, T. F. Ho, K. Maley *et al.*, 2007 Crystal structure of the kinase domain of serum and glucocorticoid-regulated kinase 1 in complex with AMPPNP. Protein Sci. 16: 2761–2769.

Communicating editor: O. Cohen-Fix